LA-UR-16-25686
Approved for public release; distribution is unlimited.

Title: Development of Techniques for Spent Fuel Assay – Differential Dieaway Final Report

Author(s): Swinhoe, Martyn Thomas
Goodsell, Alison
Ianakiev, Kiril Dimitrov
Iliev, Metodi
Desimone, David J.
Rael, Carlos D.
Henzl, Vladimir
Polk, Paul John Jr.

Intended for: Report

Issued: 2016-08-24 (rev.1)

LA-UR-16-25686
Approved for public release; distribution is unlimited.

Title: Development of Techniques for Spent Fuel Assay – Differential Dieaway Final Report

Author(s): Swinhoe, Martyn Thomas
Goodsell, Alison
Ianakiev, Kiril Dimitrov
Iliev, Metodi
Desimone, David J.
Rael, Carlos D.
Henzl, Vladimir
Polk, Paul John Jr.

Intended for: Report

Issued: 2016-07-28

Development of Techniques for Spent Fuel Assay – Differential Dieaway Final Report

Martyn Swinhoe, Alison Goodsell, Kiril Ianakiev, Metodi Iliev, Dave Desimone, Carlos Rael, Vlad Henzl, Paul Polk

Los Alamos National Laboratory

Introduction

This report summarizes the work done under a DNN R&D funded project on the development of the differential dieaway method to measure plutonium in spent fuel.

There are large amounts of plutonium that are contained in spent fuel assemblies and currently there is no way to make quantitative non-destructive assay. This has led NA24 under the Next Generation Safeguards Initiative (NGSI) to establish a multi-year program to investigate, develop and implement measurement techniques for spent fuel [1, 2, 3]. The techniques which are being experimentally tested by the existing NGSI project do not include any pulsed neutron active techniques. The present work covers the active neutron differential dieaway technique and has advanced the state of knowledge of this technique as well as produced a design for a practical active neutron interrogation instrument for spent fuel. Monte Carlo results from the NGSI effort show that much higher accuracy (1-2%) for the Pu content in spent fuel assemblies can be obtained with active neutron interrogation techniques [4, 5] than passive techniques and this would allow their use for nuclear material accountancy independently of any information from the operator.

The main purpose of this work was to develop an active neutron interrogation technique for spent nuclear fuel. The primary motivation for the NGSI initiative was to improve the capability of international and national regulatory agencies to independently verify the plutonium mass in, and detect the diversion of pins from, spent commercial fuel assemblies. The four primary safeguards needs that are addressed by the researched technologies are the following: (1) Recovery from a loss of the Continuity-of-Knowledge. (2) Verification of the plutonium input accountability mass at a (re)processing facility, (3) Quantification of the Pu mass shipped from one facility to another in the context of resolving shipper/receiver differences. And (4) enabling the termination of safeguards at a spent fuel repository.

The measurement of plutonium in spent fuel is not an easy problem because of the complex combination of fissile, fertile, neutron emitting and gamma emitting nuclides of which it is composed. Currently the techniques that are applied to the measurement of spent fuel by IAEA inspectors are the Digital Cerenkov Viewing Device (DCVD) [6], which measures photons produced by radiation from fission products, and the Fork Detector [7] which measures the gamma emission from fission products and the neutron emission originating primarily from curium. From these measured signatures, burnup codes can infer plutonium mass. (The Safeguards MOX Python Detector (SMOPY) [8] detector is an addition to this suite of

instruments; it is similar to the Enhanced Fork detector with the addition of a burnup code integrated with the hardware). Neutron generator based systems are used for waste measurement (dissolved hulls) in reprocessing plants as well as in general waste drum analysis. Such DDA systems have been used for decades but have never been applied to the assay of complete spent fuel assemblies, which represent a much more highly multiplying system than waste with correspondingly more complex behavior. Figure 1 shows the time behavior of traditional DDA used for waste [9]. The information from this system is obtained 500 μs or more after the neutron pulse. Figure 2 shows the signal behavior for the spent fuel DDA system in comparison. The interrogation is complete before 500 μs has elapsed after the pulse.

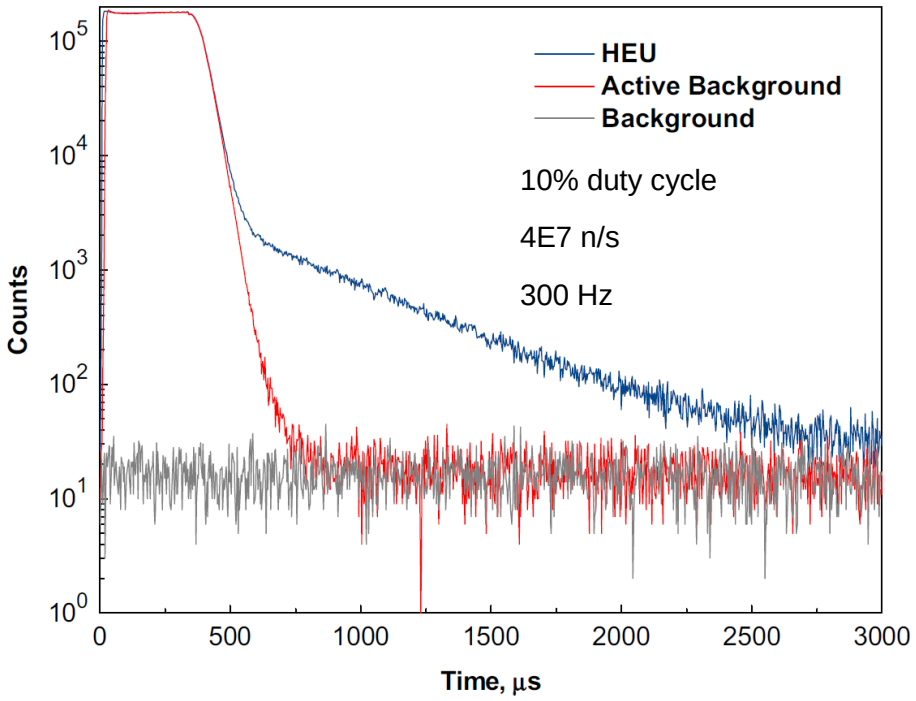

Figure 1 Time Behavior of Traditional DDA signals (as in waste measurement)

The objective of this work was to advance the development of the DDA by experimentally demonstrating its feasibility and improving performance. The results of this work have already been incorporated into the design of a practical DDA system being built under the NSGI Spent Fuel Project.

This report gives an overview of the work and presents the conclusions that have been drawn. Further details can be found in the list of references resulting from this work, listed in Appendix A.

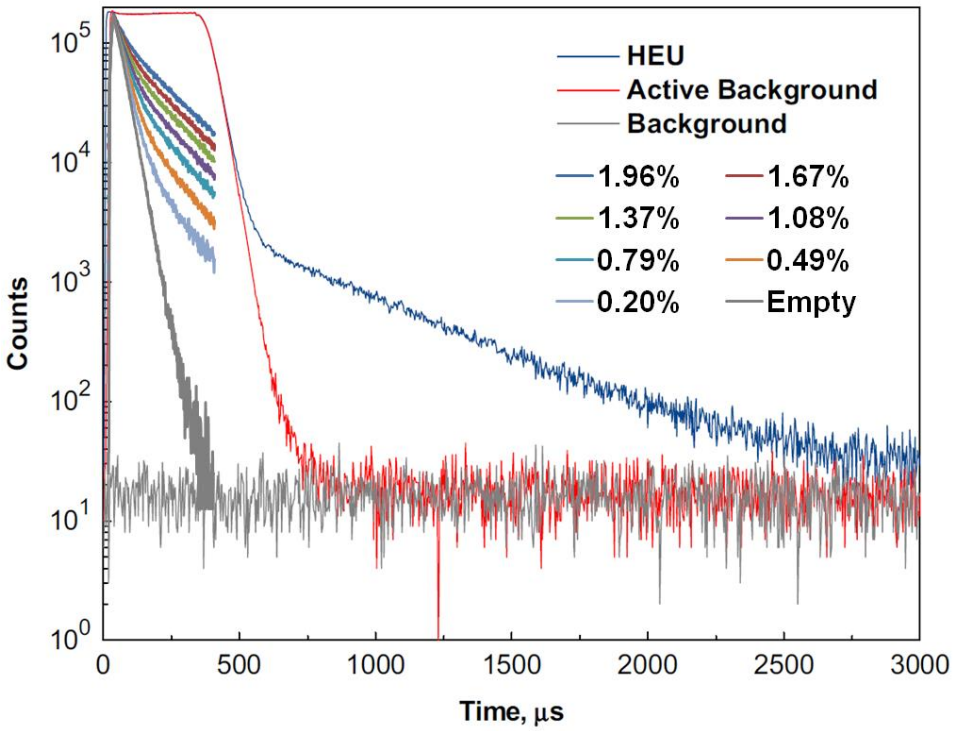

Figure 2 Time Behavior of Fuel Assembly DDA in Comparison with Traditional DDA

Background

The Differential Die-Away (DDA) instrument uses neutron pulses from a 14-MeV neutron generator to interrogate the fuel assembly. The interrogating neutrons will induce fission in the fissile isotopes present in the assembly (e.g. ^{235}U, ^{239}Pu, ^{241}Pu, etc) and the resulting induced fission rate will decay with a characteristic die-away time of the order of 100 μs. The time correlated neutrons from the induced fissions are analyzed as a function of time after the neutron pulse to determine the fissile content in the sample. Previous MCNPX calculations [5] have shown there is valuable information in the DDA signal at short times after the initial pulse. Combinations of the passive neutron signal with DDA results from different time windows can lead to estimates of plutonium mass with uncertainty in the range 1-2% when the cooling time can be determined by a separate method (for example passive gamma). Figure 3 shows the geometry of a spent fuel measurement instrument. The current modeling has used ^{3}He tubes as neutron detectors, which are shielded by a large amount of lead to reduce the gamma background from a spent fuel assembly. These detectors were chosen in order to have a reasonable efficiency for the detection of delayed neutrons in a combined DDA & delayed neutron instrument. The neutron tube is surrounded by tungsten and steel to 'tailor' the spectrum that is incident on the spent fuel. Figure 4 shows the neutron counting rate as a function of time after the external neutron burst for PWR fuel with different burnup.

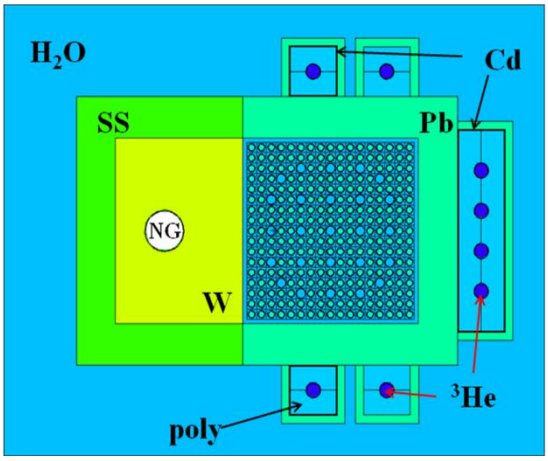

Figure 3 Monte Carlo Geometry of Simulated DDA Instrument

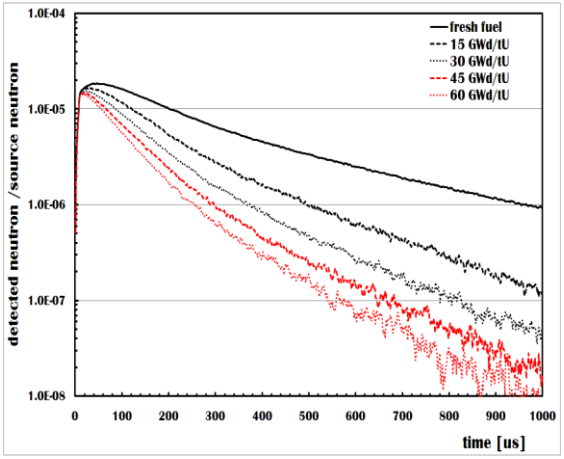

Figure 4 Time Response of Neutron Count Rate following an External Neutron Burst for assemblies with different Burnup

The simulations also show that in general the counts in a given time window are functions of the main characteristics of the fuel assembly, initial enrichment, burn-up and cooling time. However for particular time windows the relationship between the count rate and the effective ^{239}Pu content is much less dependent on these parameters. This is shown in figures 5 and 6 for time windows of 0-50μs and 500-1000μs respectively. These simulations, and on-going development of analysis algorithms under NA241 funding, indicate that DDA provides an information-rich signal from which we can extract the significant parameters of the fuel assembly.

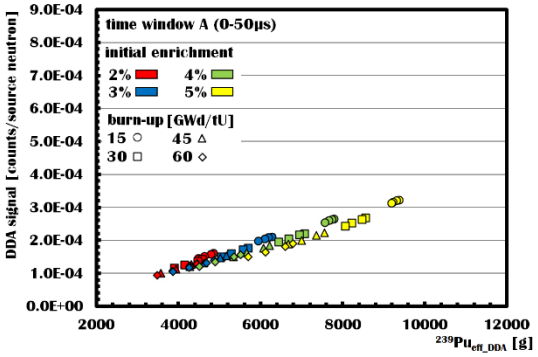

Figure 5 DDA Response to Different Fuel Assemblies in the time window 0-50 μs

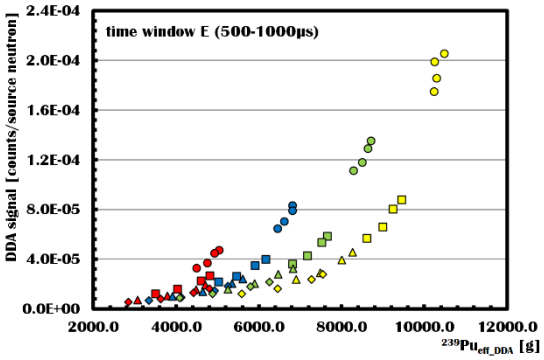

Figure 6 DDA Response to Different Fuel Assemblies in the time window 500-1000 μs

Technical Approach

A mock-up of the DDA instrument has been built and tested at LANL using the PWR 15x15 fresh LEU fuel assembly. The Thermo Scientific P 385 DT neutron generator (Figure 7) produces 14 MeV neutrons from DT reactions in a pulse that is about 20 μs long. In these experiments the duty cycle is 5% and so the repetition frequency is 2.5 kHz. The output is about 2×10^8 n/s, approximately independent of the chosen duty cycle. This is different from the previous generation of pulsed DT tubes which had a 10 μs wide pulse and a frequency of 100Hz.

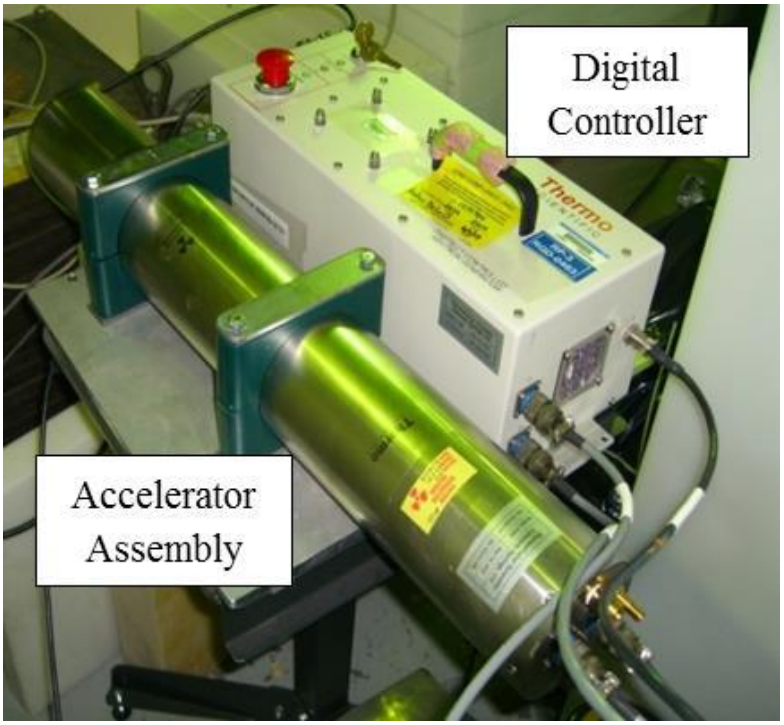

Figure 7 Neutron generator tube and control box

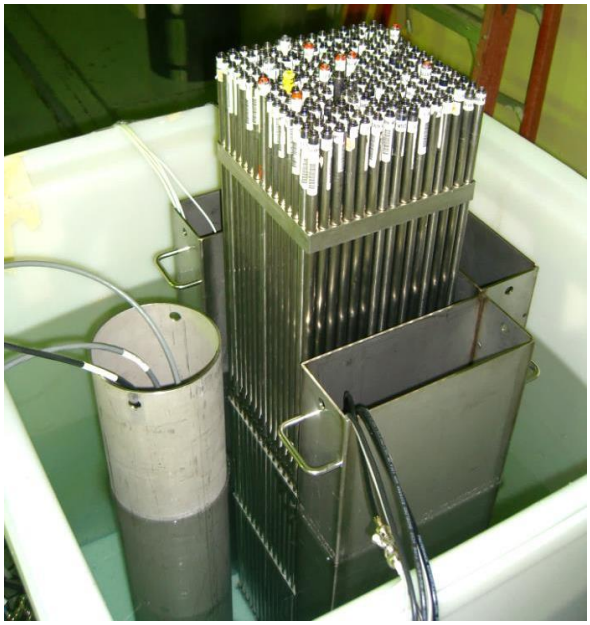

Figure 8 Mock-up fuel assembly in the center of the water tank surrounded by detector and neutron generator pods

The experimental arrangement is shown in Figure 8. Each of the detector pods (on three sides) held three ^{3}He detectors, wrapped in 23.5 mm thick poly sleeves and covered with cadmium. Figure 9 shows a Monte-Carlo diagram of the setup. Note the numbering of the detectors, which will be extensively referred to in the following sections.

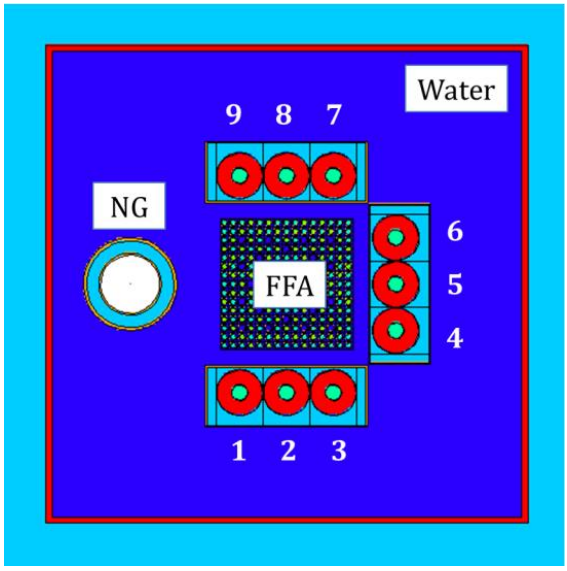

Figure 9 MCNP model of water tank experiment

Figure 10 shows the data acquisition system and storage for the list mode data. The acquisition was done using National Instrument cards with LabView software developed under the related NA-24 spent fuel project. Data analysis software was written to handle the list mode data files.

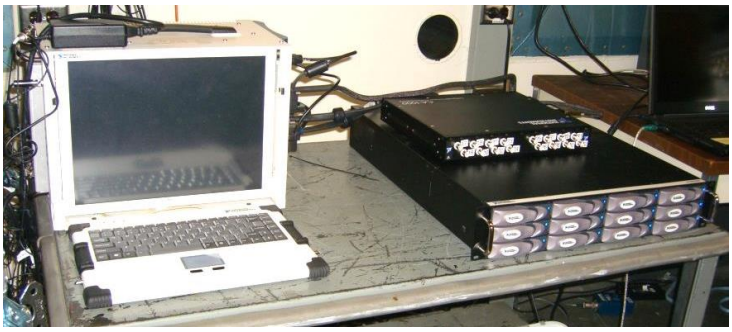

Figure 10 Data acquisition system and 2 Tb RAID storage system

The mock-up fuel assembly is made up of a combination of individual fuel rods of LEU, DU and poison pins, depending on the experiment (Figure 11). The average enrichment ranged from DU to 1.96%, which covers the range expected in spent fuel assemblies.

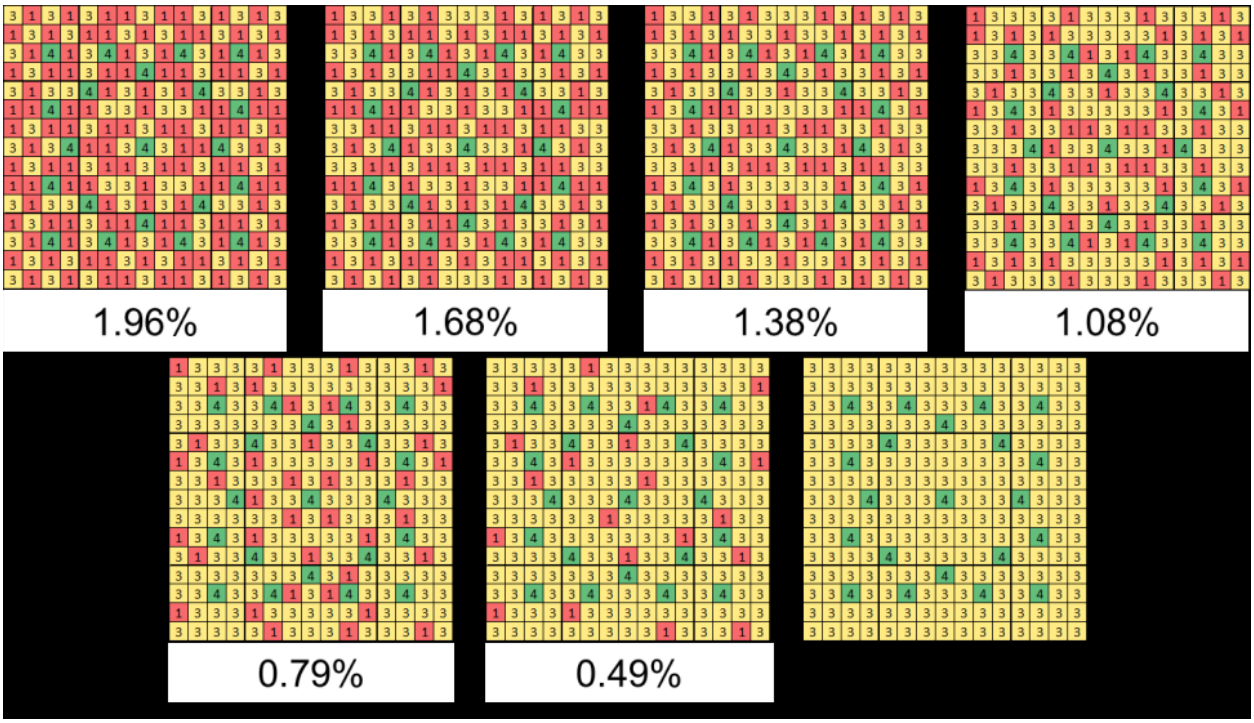

Figure 11 Individual rod combinations used to vary the average enrichment (red=LEU, yellow=DU and green=guide tube)

Results

Electronics and Deadtime

Time-dependent spatial data were collected from the nine ^{3}He neutron detectors with PDT pre-amplifiers (models 10A and 20A). In addition, an advanced, faster recovery detector/electronics package (KM detector) was tested. The KM detector and the PDT Detector 1 were positioned symmetrically around the fuel assembly and neutron generator. The neutron generator was operated at three intensities (high, medium, low) to test the count rate limits of the detectors.

The DDA count rate recorded by the nine ^{3}He detectors, especially in the early time domain (less than 100 μs), was high. We performed conventional deadtime correction of the data using the infinite exponential deadtime correction method given in Eq. (1), where $\dot{S}_{DT}$ is the deadtime corrected count rate, $\dot{S}_M$ is the measured count rate, and d is the deadtime correction coefficient.

$$\dot{S}_{DT} = \dot{S}_M \cdot \exp(d \cdot \dot{S}_{DT}) \cong \dot{S}_M \cdot \exp(d \cdot \dot{S}_M \cdot \exp(d \cdot \dot{S}_M \cdot \exp(d \cdot \dot{S}_M \cdot \exp(d \cdot \dot{S}_M \ldots)))) \quad (1)$$

The deadtime correction coefficient for the ^{3}He detectors with PDT pre-amplifiers was determined to be ~1.5 μs, per detector, whereas d for the KM detector was ~0.45 μs. The DDA signal is plotted in Figure 12 for Detector 1 and the KM detector for three different NG intensities. The figure shows in solid lines the deadtime corrected results for the three intensities. (The lower two intensity results from both detector types overlap). At the highest intensity it can be seen that

the KM electronics deadtime corrected results look a reasonable shape, whereas the deadtime corrected detector 1 results cannot be corrected in a reasonable way. This is attribute to non-linear saturation effects at these count rates. (The dotted curves show the highest intensity raw results for each detector before deadtime correction). Due to its predictable behavior and shorter dead-time, the advanced KM detector performed better than Detector 1 especially during the time period directly after the NG pulse when highest count rates were recorded. More details of this work can be found in references A.8, A.16 and A.19.

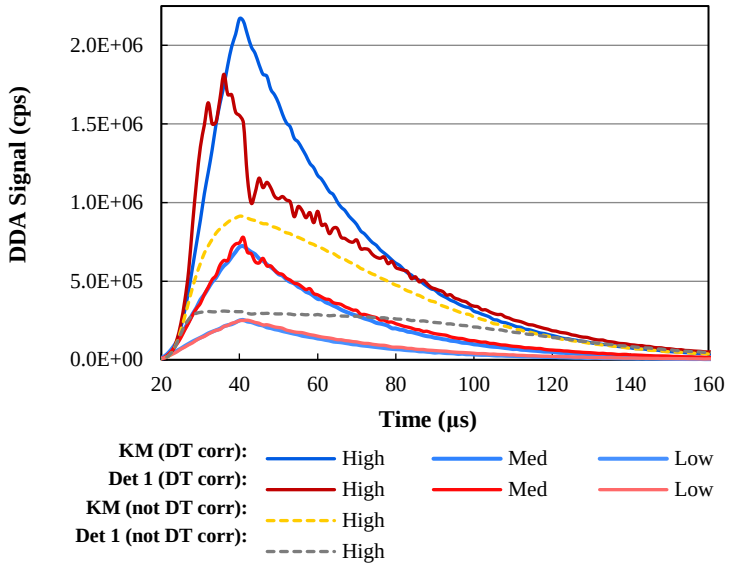

Figure 12 The PDT detector 1 and advanced KM detector electronics were tested in symmetric positions around the FFA for three neutron generator intensities (high, medium, low). The deadtime corrected (DT corr) and non-DT corrected signals are plotted. The Detector 1 electronics were able to withstand the high count rates directly after the NG pulse, except the very high intensity pulse. The KM curve shows the expected DDA signal behavior even at high NG intensity.

Neutron Generator Output

The neutron output of the generator was measured using Nb foils in accordance with ASTM E496. The reaction is ^{93}Nb(n,2n)^{92m}Nb with the subsequent emission of a 934.4 keV gamma with a half-life of 10.15 days. At 14 MeV the cross-section is 1.356 barns and does not vary much with energy in this region. The calibration was performed in continuous (100% duty factor) mode and at 10% duty factor and 2500Hz. The generator was operated at 70 µA and 125 kV for both modes and the flux monitor detector acquired data during pulsed mode calibration. The niobium foils were 10-mm diameter and 0.1-mm thick. Two niobium foils were placed on each side of the generator for each mode of operation. The activity was measured with an Ortec Detective gamma detector calibrated with a ^{152}Eu source. The result of the efficiency calibration is shown in Figure 13.

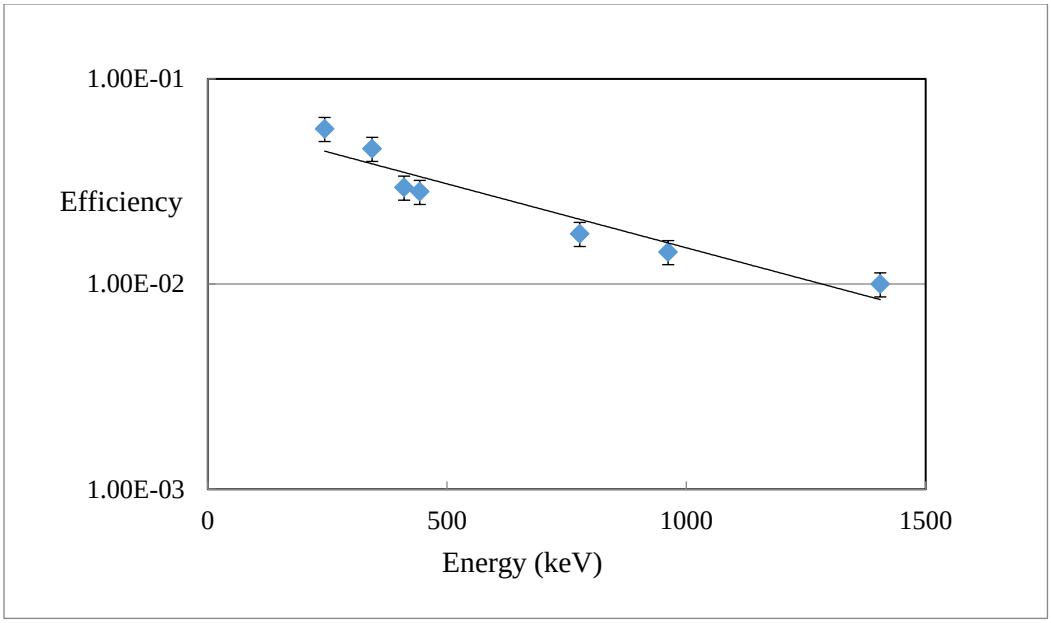

Figure 13 Gamma detector Efficiency Measured with 152Eu source

When the generator was run at 70 µA and 125 kV and pulsed at 10% duty factor and 2500 Hz, two measurements gave $2.7 \cdot 10^8$ n/s ± $1.3 \cdot 10^7$ n/s and $2.6 \cdot 10^8$ n/s ± $1.2 \cdot 10^7$ n/s. With the same parameters but with the tube running continuously, the results were $1.9 \cdot 10^8$ n/s ± $3.8 \cdot 10^7$ n/s and $2.0 \cdot 10^8$ n/s ± $4.0 \cdot 10^7$ n/s.
There are some peculiarities of the neutron generator operation. The output substantially increases from a 5% duty cycle to a 10% duty cycle, whereas the pulse width is the same (20µs) for 5% and 10% duty cycle.
A complex wide (or inter laboratory) comparison of neutron generator strength measurement would be a useful exercise.

Simulation

The DDA instrument design used in the simulations with the Monte Carlo N-Particle code [10] mimics the major components of the experimental design as closely as possible, including the detector dimensions, fresh fuel rod arrangement, stainless steel enclosure positions around the assembly, the water tank level, and the distance between the NG and the fuel assembly (Figure 9). Other materials surrounding the tank and the effects from room-return in the shielded cell are considered negligible.

Multiple MCNPX simulations of the DDA instrument were modeled with variations in the setup in order to determine the sensitivity of the results to the modeling parameters. These variations included detector position, Cd thickness, water thickness between the fresh fuel assembly and neutron generator, distance between the detector pods and the fresh fuel assembly, and vertical position of the ^{3}He detectors inside of the pods.

Experimental Results and Comparison with Simulation

Figure 14 shows the measured DDA signal as a function of enrichment. Figure 16 and Figure 17 show the measured and simulated dieaway and their relative differences as a function of enrichment for the interval 70 -100 μs. In general, the relative differences decrease with increasing enrichment and hence neutron multiplication. Detector 1 is affected by both deadtime and a greater contribution of neutrons directly from the neutron generator.

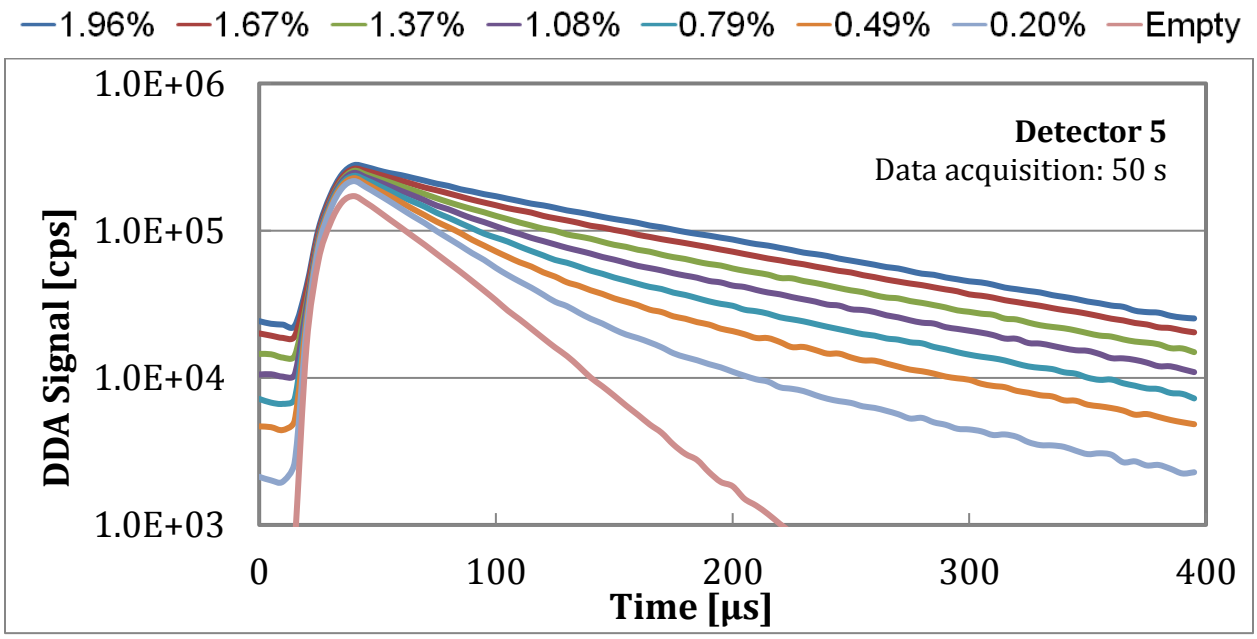

Figure 14 Time spectra from different enrichment mock-up assemblies

Figure 17 and Figure 18 show the same data for the interval 100 -150 μs. For this interval there appears to be no systematic trend with enrichment and the biggest differences come from the empty case.

Figure 19 and Figure 20 show the 'Empire State' shape of the dieaway times for the measurements and simulations respectively. We can infer the enrichment from the shape of these results without requiring an absolute measurement of the flux.

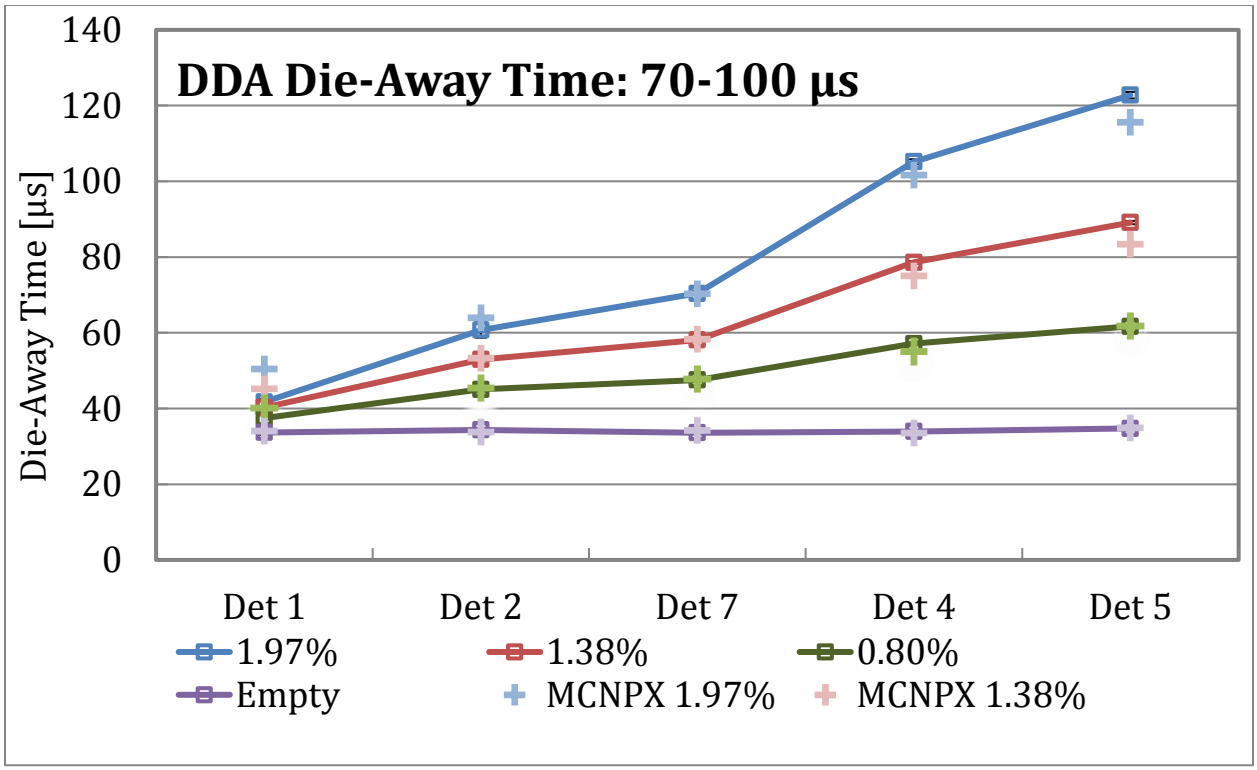

Figure 15 Dieaway times of different detectors for various enrichments (70-100µs)

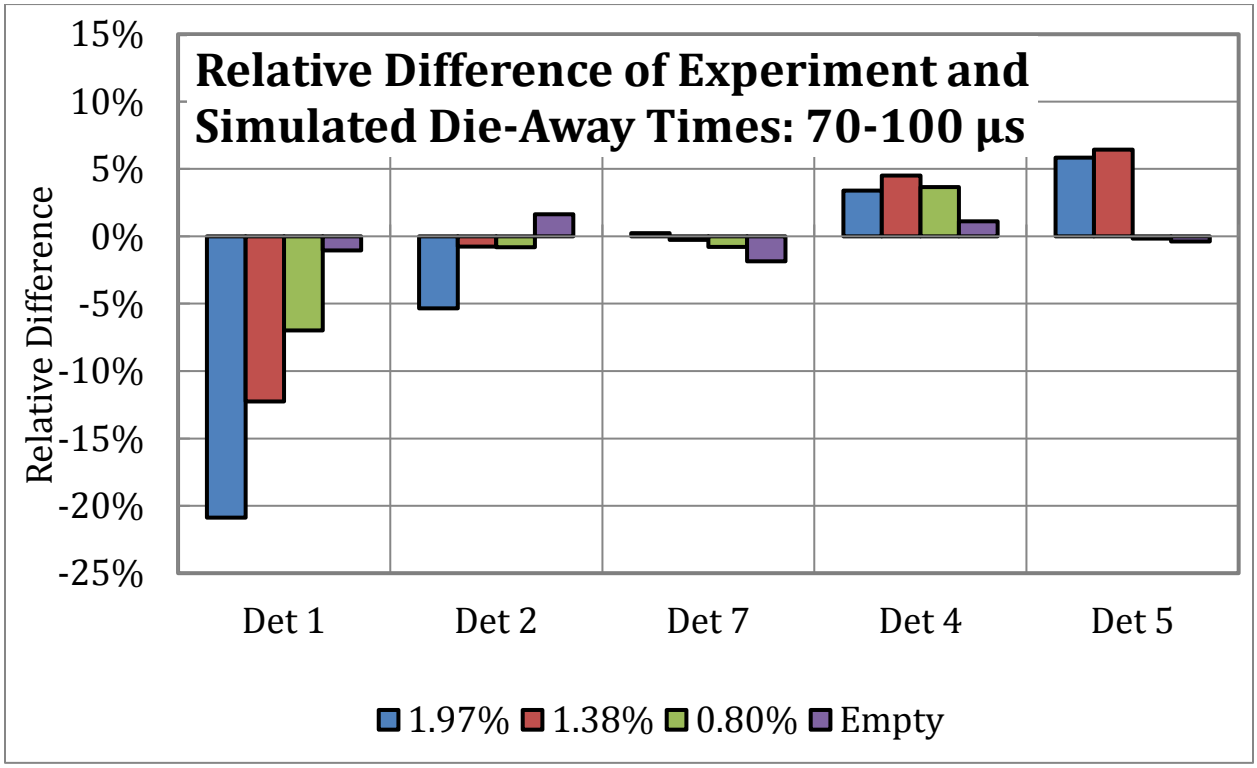

Figure 16 Relative differences between calculated and measured dieaway times (70-100µs)

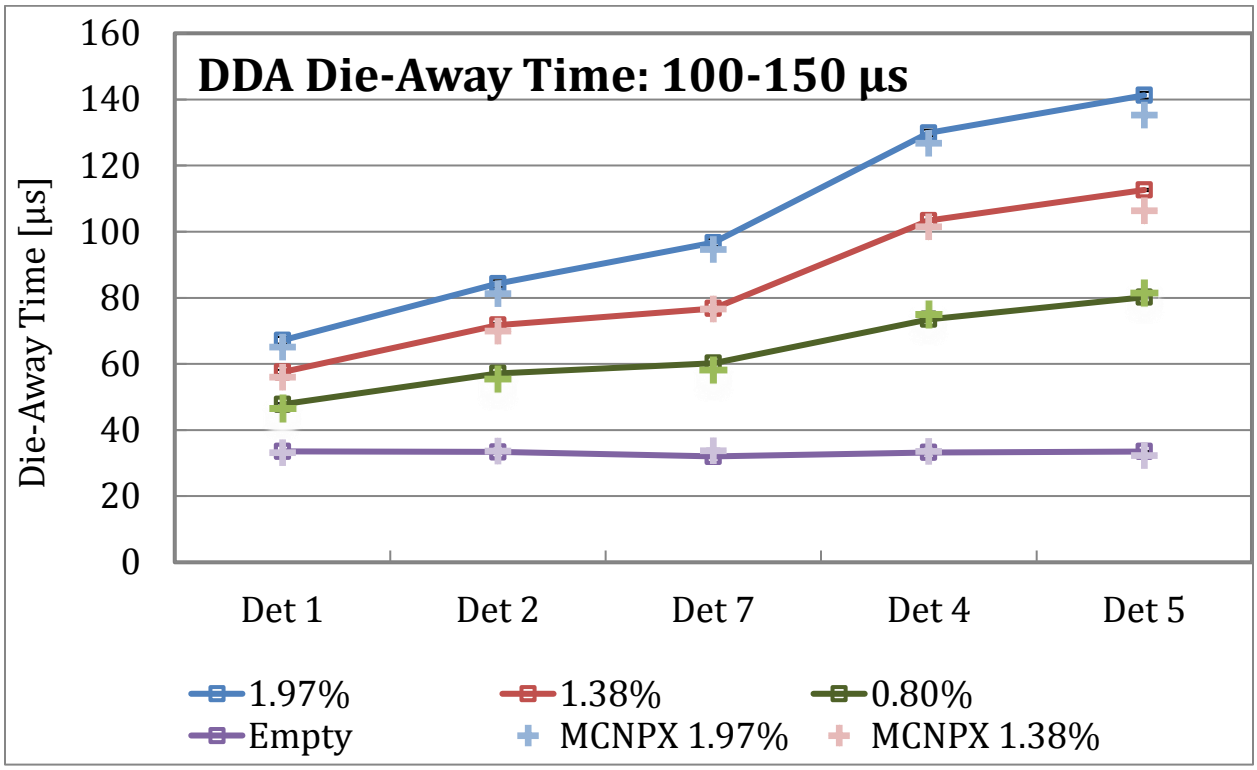

Figure 17 Dieaway times of different detectors for various enrichments (100-150µs)

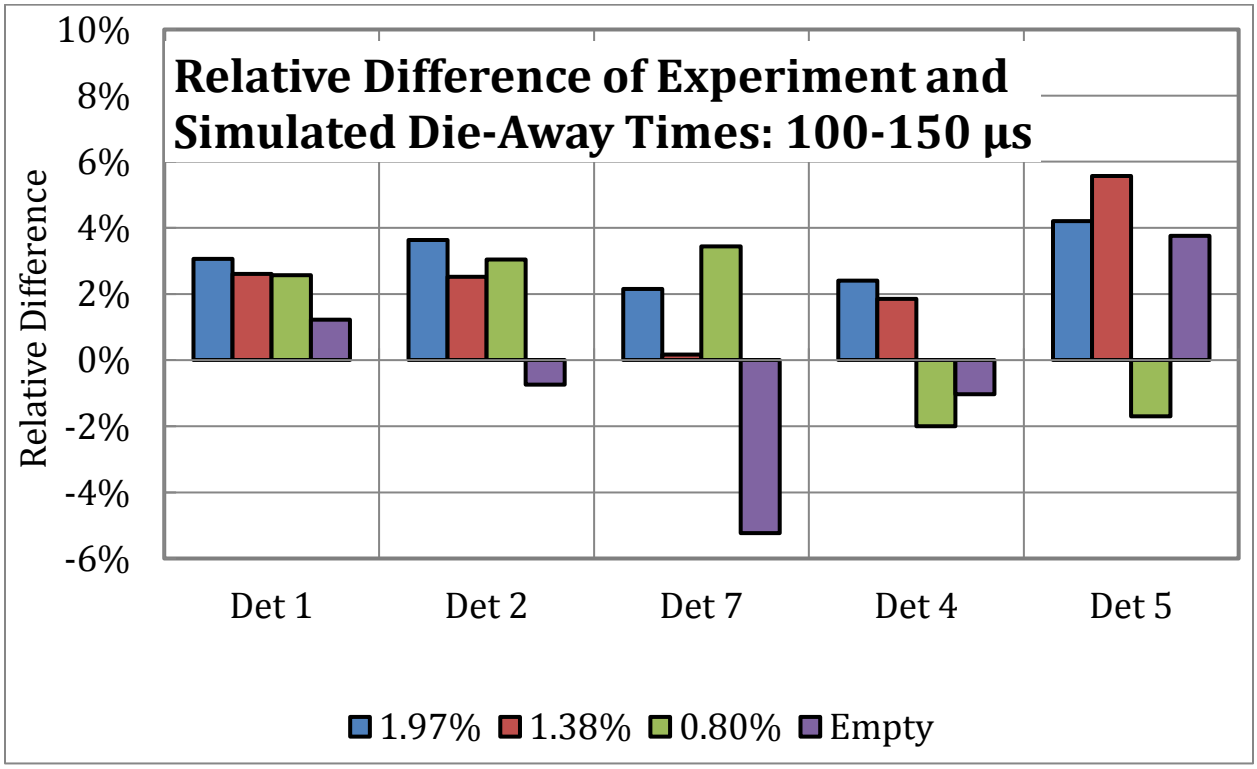

Figure 18 Relative differences between calculated and measured dieaway times (100-150µs)

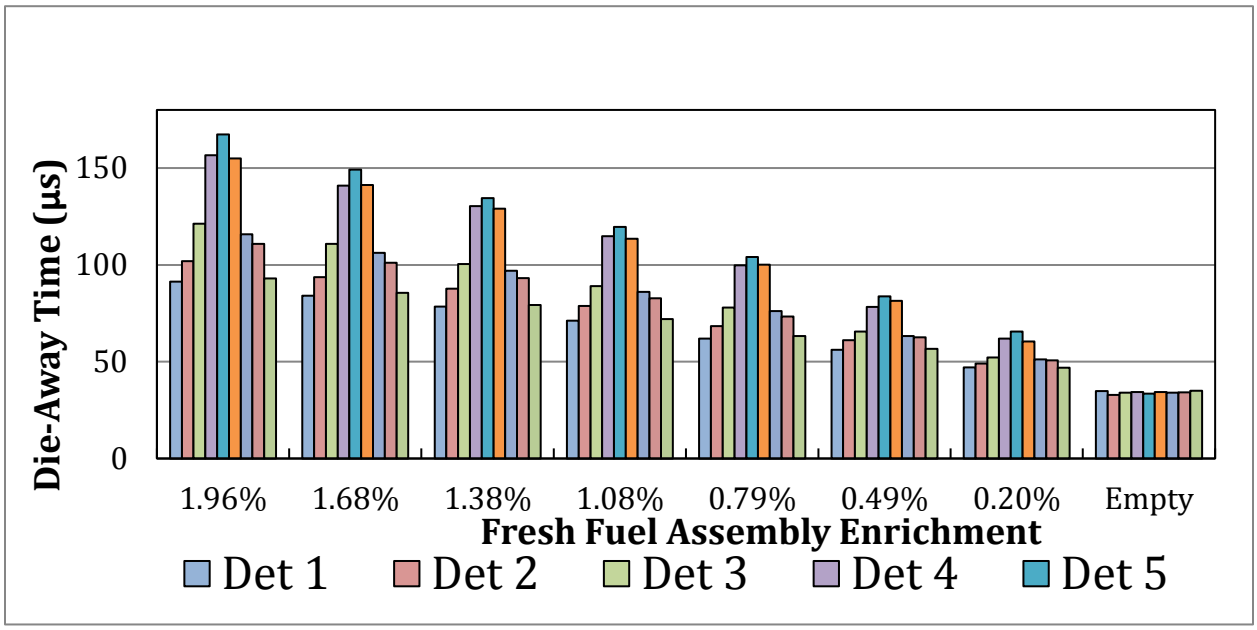

Figure 19 Experimental DDA Signal Die-Away Times in 100-200 µs Time Domain

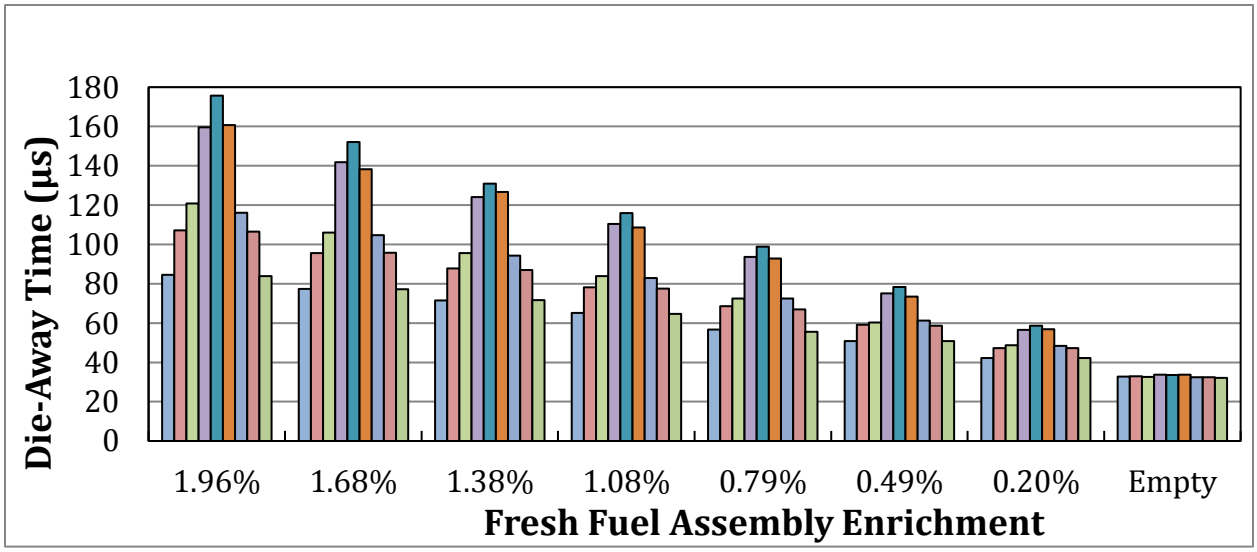

Figure 20 Simulated DDA Signal Die-Away Times in 100-200 µs Time Domain

The uncertainty in the experimentally determined die-away times was estimated by recording a series of 10 measurements each 30 s for two fresh fuel assembly configurations with different average enrichments (1.67% and 1.09% ^{235}U) and the empty assembly without any fuel pins. For the empty fuel assembly, the DDA signal die-away time depends on the detector system properties, such as the amount of moderating material around the detectors. For each measurement, we determined the die-away time value in the 70-100 µs, 100-150 µs, and 150-200 µs time intervals which were chosen to minimize the dead time effects and maximize the

statistical significance of the recorded data. The mean die-away time and the absolute and relative standard deviation (σ) are listed in Table 1. Overall, for the early and mid-time domains evaluated the experimental die-away times generally deviated by less than 1.0 μs, or less than 1.0%, from the mean. In the later time domain, we found larger relative errors due to decreasing count rates. Averaged over all sixty measurements, the standard deviation of individual measurement is approximately 1.0%. Based on these results, and considering typical uncertainties associated with various experimental procedures (calibration, position reproducibility) cited in previous work [A.18] we concluded that in the case of fresh fuel, a measurement time of 30 s was sufficient for a statistically accurate die-away time determination in the early to mid-time (<150 μs) domains. In practice, we exceed this minimum limit and acquire data for upwards of 5-10 min.

Table 1 The results of ten 30 s measurements: the die-away time in three time domains, the mean value, standard deviation (σ), and relative uncertainty were determined for three fresh fuel cases (1.67%, 1.09%, and 0.49% 235U) and the empty setup. The relative error gradually increased as the fissile mass in the assembly decreased.

	Die-Away Times [μs]								
Run	70-100 μs			100-150 μs			150-200 μs		
(30 s)	1.67%	1.09%	Empty	1.67%	1.09%	Empty	1.67%	1.09%	Empty
1	64.47	51.41	33.69	85.90	66.92	32.36	117.83	101.60	32.90
2	64.93	51.47	33.79	84.27	67.56	32.67	116.50	98.67	32.29
3	64.39	51.90	33.88	85.20	67.57	32.78	114.39	97.71	32.07
4	64.70	51.70	34.33	86.10	67.77	32.35	115.45	98.19	32.16
5	64.25	52.05	34.04	85.16	66.50	32.14	119.92	96.79	32.88
6	63.94	52.50	34.19	87.19	67.32	32.59	117.30	98.93	33.30
7	65.66	52.32	33.17	84.69	67.21	32.14	118.07	96.59	32.17
8	63.75	51.72	33.61	84.81	67.36	32.54	116.19	96.70	32.08
9	63.93	51.11	33.52	85.83	66.29	32.31	116.52	97.33	31.77
10	63.53	52.28	33.89	85.16	67.01	32.43	115.65	98.21	32.46
Mean [μs]	64.36	51.85	33.81	85.43	67.15	32.43	116.78	98.07	32.41
σ [μs]	0.63	0.45	0.34	0.85	0.48	0.21	1.57	1.49	0.48
σ [%]	1.0%	0.9%	1.0%	1.0%	0.7%	0.7%	1.3%	1.5%	1.5%

Effect of Gd Poison Rods

One significant difference between the spent fuel, which is the target of this development, and the fresh fuel used in these experiments, is the presence of thermal neutron absorbers, originating as fission products. In order to extend the parameter space investigated here by measurement and calculation, thermal neutron absorbers, in the form of Gd doped fuel rods, were added to the assembly.

Twelve Gd poison rods were positioned uniformly throughout the fuel assembly for each enrichment (Figure 21). The time-dependent DDA signal was reconstructed from the list-mode data (Figure 22). The presence of 12 Gd poison rods positioned uniformly throughout the assembly caused the neutron population to decrease, which reduced the number of neutron generations, thereby decreasing the DDA signal die-away time magnitudes (Table 2). For the highest enriched case of 1.68% ^{235}U, the die-away time of the DDA signal in the front three detectors (Detectors 1, 8, and 3) decreased by approximately 12% in the 70-100 μs time domain when the 12 Gd rods were inserted uniformly in the fuel assembly. (For detector positions, see Figure 9) From DDA spent fuel simulations, the die-away time in the 100-200 μs time domain decreased by approximately 50% between a fresh and fully burned (50 GWd/tU) fuel assembly. Therefore, the 12% decrease in die-away time in the fresh fuel experiments with and without Gd poison rods roughly corresponds to a 10 GWd/tU burnup. The change to the die-away time of the front detectors lessened as the enrichment of the fuel assembly decreased, but there was still a noticeable change for the 0.80% and 0.22% ^{235}U configurations.

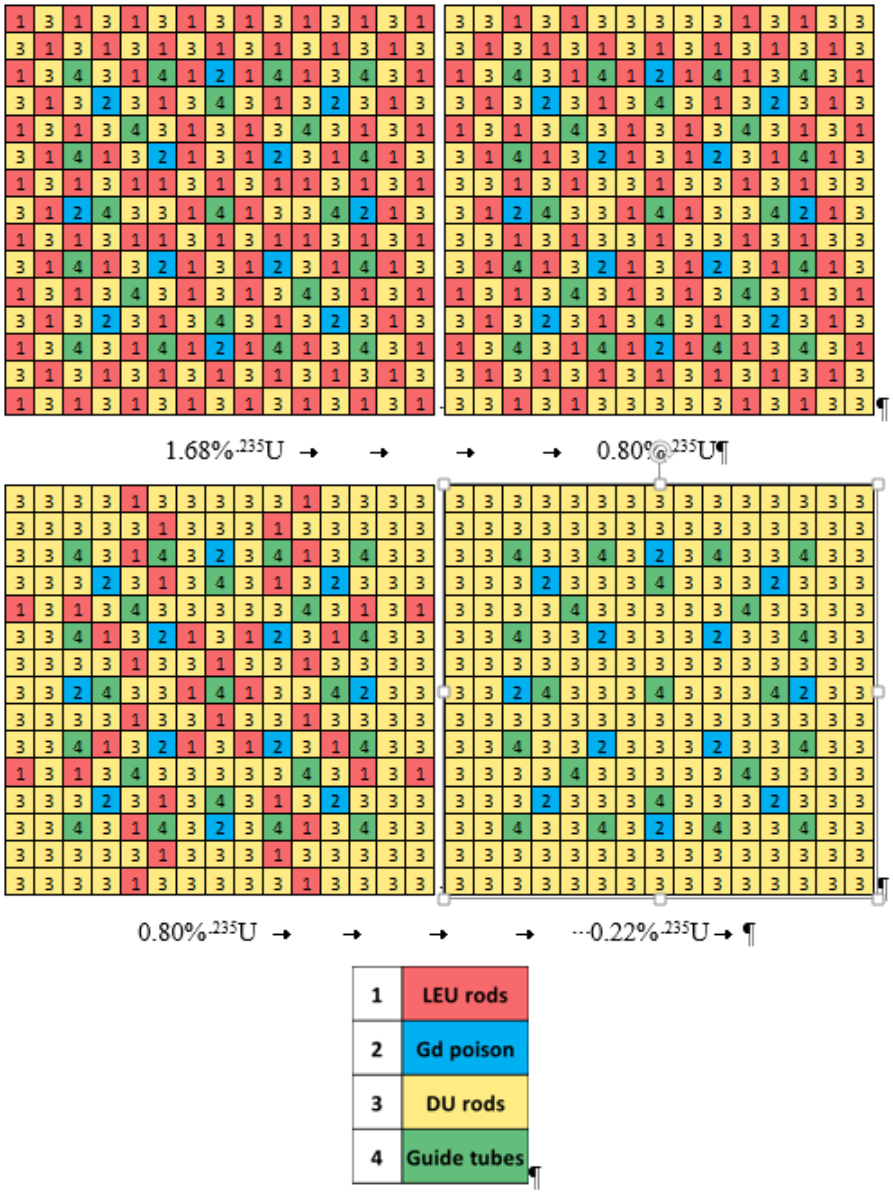

Figure 21 Four fresh fuel enrichments with 12 Gd rods were used during the experimental campaign.

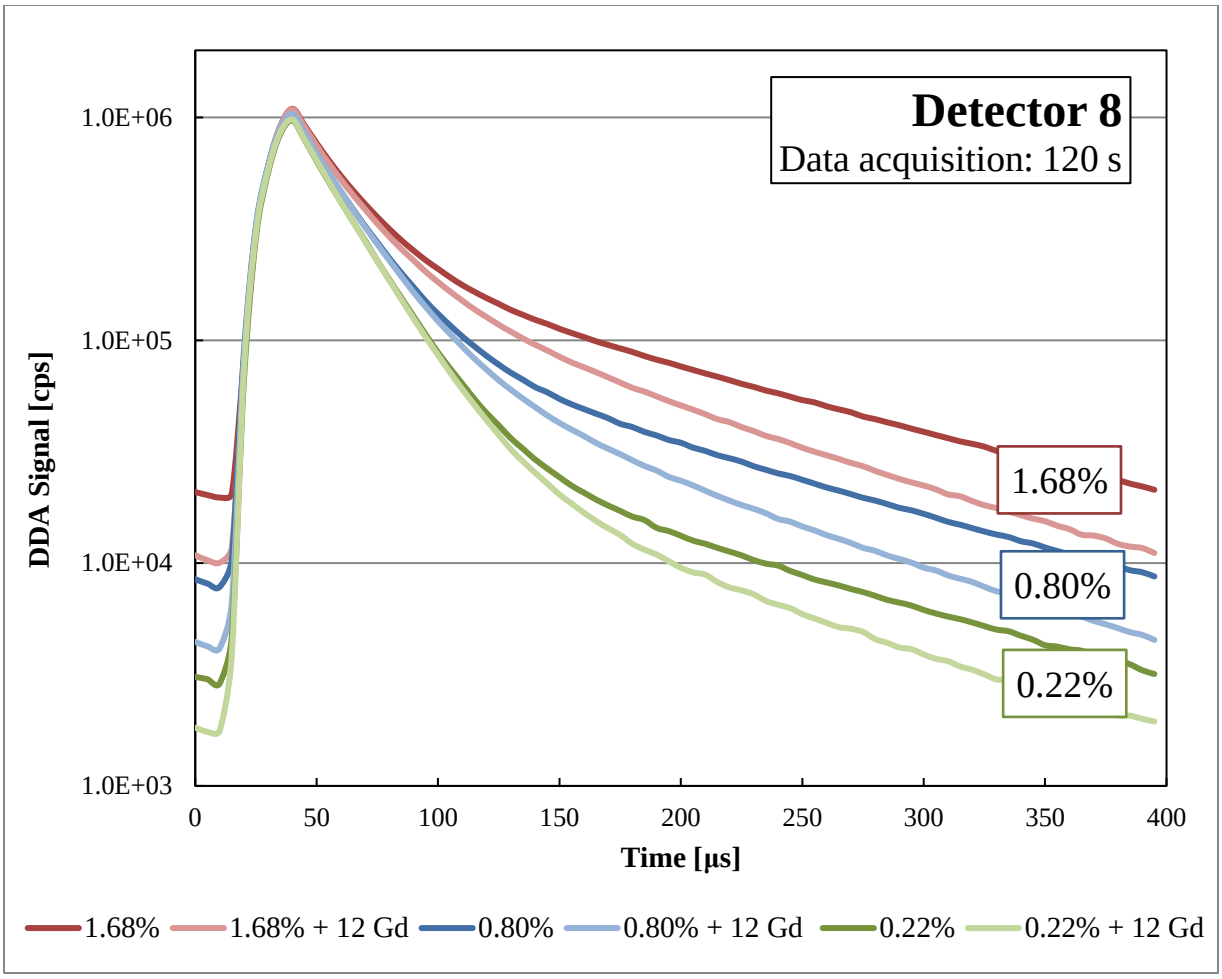

Figure 22 Experimental data comparing the DDA signal for three enrichments (1.68%, 0.80%, and 0.22% ^{235}U) with and without twelve enriched poison (Gd) rods.

Table 2 The experimental DDA signal die-away time in the 70-100 µs time domain was determined for Detectors 1, 8, and 3 for three fresh fuel enrichments (1.68%, 0.80%, and 0.22% 235U) and the empty case.

	Experimental Data 70-100 µs Time Domain Die-Away Times [µs]						
	1.68%		0.80%		0.22%		Empty
	No Gd	12 Gd	No Gd	12 Gd	No Gd	12 Gd	No Gd
Detector 1	36.6	33.1	25.7	23.9	19.9	19.3	15.7
Detector 8	44.9	40.1	33.0	30.8	26.1	25.5	22.1
Detector 3	No data	43.4	34.8	32.2	26.9	26.0	22.4

MCNPX simulations of the experimental setup were performed for a range of fresh fuel enrichments, with and without Gd poison rods. The time-dependent DDA signal of the fresh fuel assembly with and without 12 Gd rods is shown in Figure 23. The die-away time of the simulated DDA signal was determined for multiple detector positions and fuel enrichments, with and without Gd rods (Table 3).

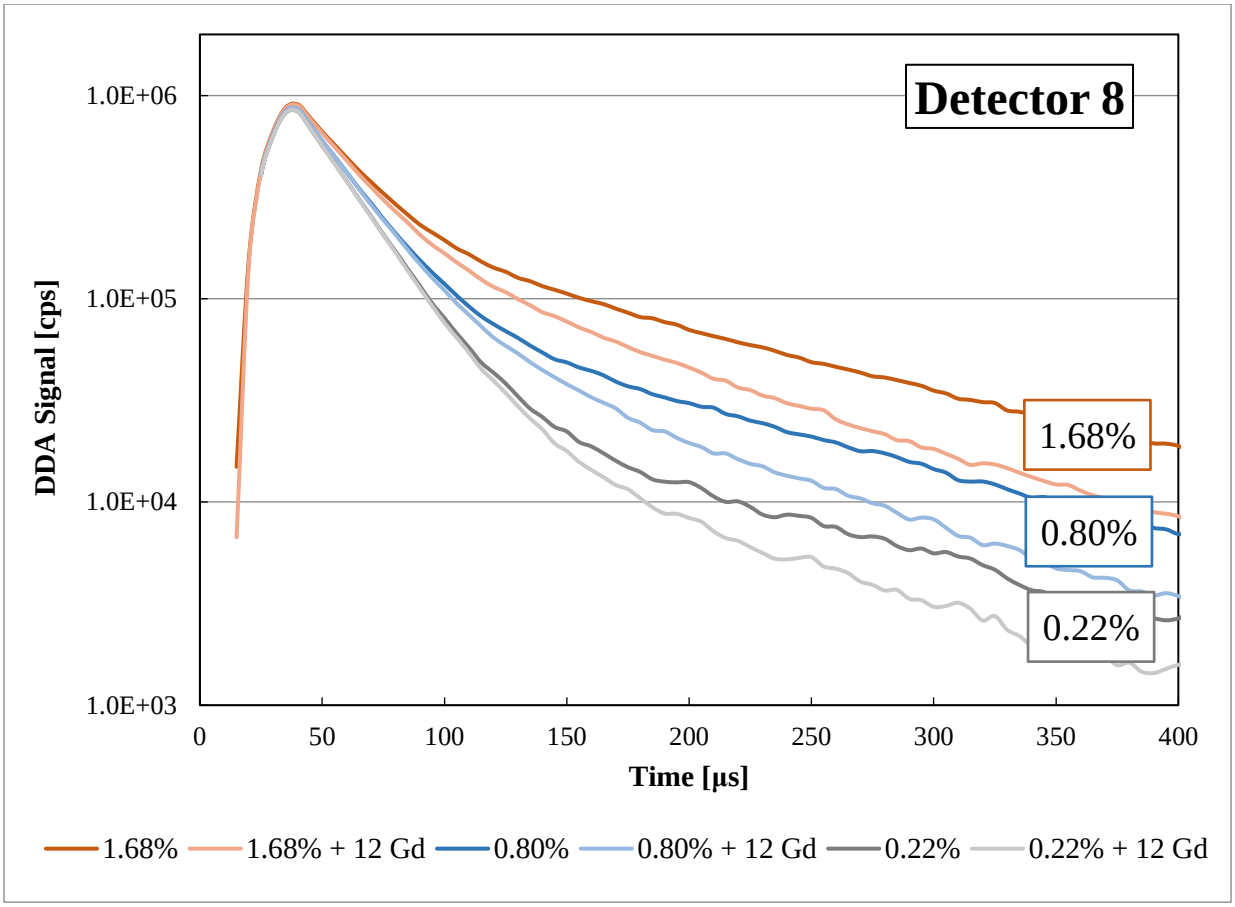

Figure 23 Simulated results of the DDA signal for three enrichments (1.68%, 0.80%, and 0.22% ^{235}U) with and without twelve enriched poison rods (Gd).

Table 3 The simulated DDA signal die-away time in the 70-100 µs time domain was determined for Detectors 1, 8, and 3 for three fresh fuel enrichments (1.68%, 0.80%, and 0.22% 235U) and the empty case.

	MCNPX Simulation 70-100 µs Time Domain Die-Away Times [µs]						
	1.68%		0.80%		0.22%		Empty
	No Gd	12 Gd	No Gd	12 Gd	No Gd	12 Gd	No Gd
Detector 1	36.9	32.7	25.9	23.9	20.0	19.3	15.5
Detector 8	45.2	39.6	33.4	30.9	26.1	25.0	21.6
Detector 3	48.0	40.8	33.9	31.2	25.9	25.2	21.3

Qualitatively, the time-dependent behavior of the DDA signal from simulation and experiment trends well for multiple enrichments (Figure 24). The discrepancies may be due to the presence of delayed neutrons which were not simulated in MCNPX due to the time cutoff of the tally. The delayed neutrons would affect the relative magnitude of the DDA signal, producing a greater effect in the later time domains.

The relative differences of the die-away times of the DDA signal in the 70-100 µs time domain from the experimental data and simulation results are compared in Figure 25. On average, the

relative difference between the experimental and simulated die-away times in the 70-100 μs time domain was ±2%.

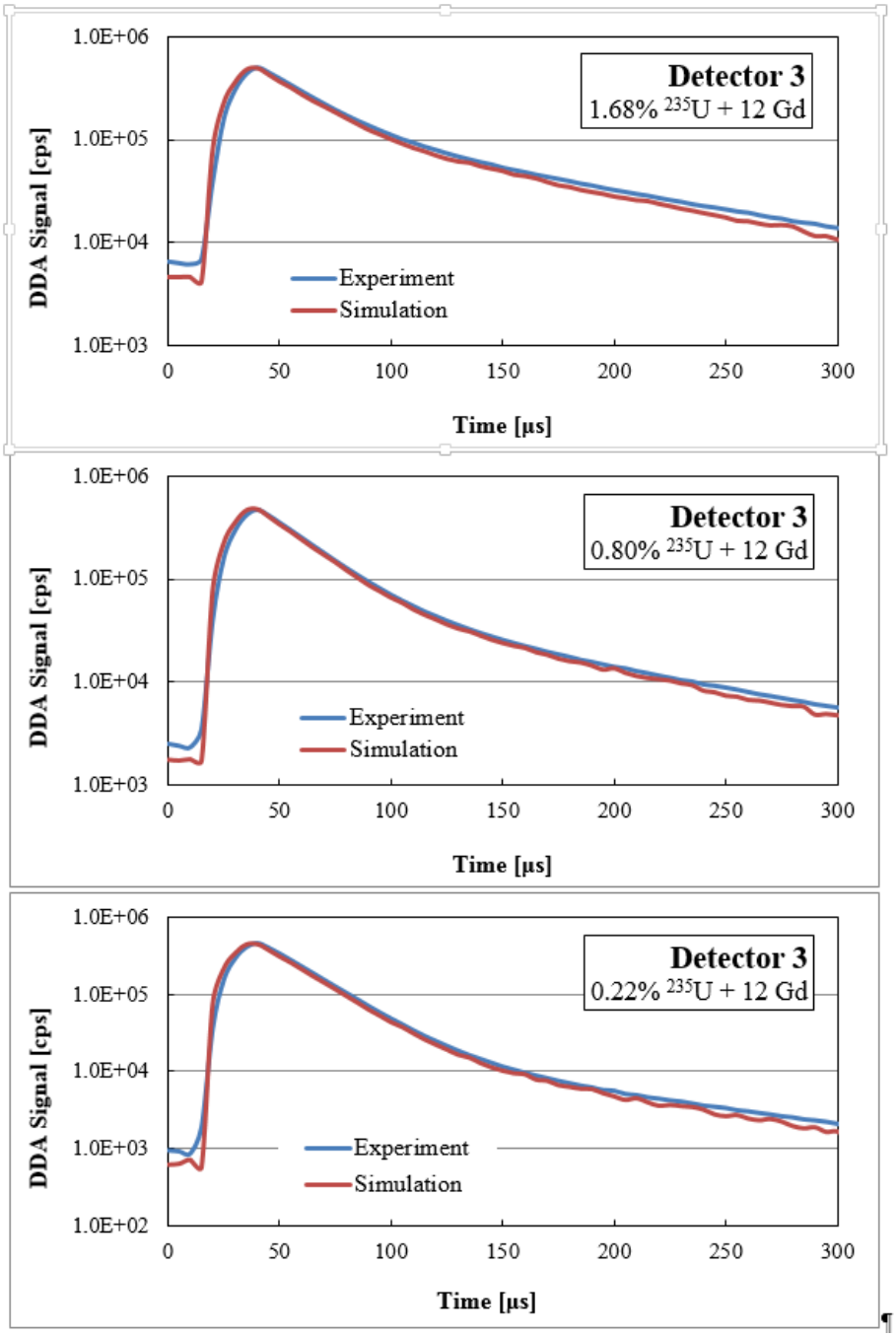

Figure 24 The measured and simulated time-dependent signal from Detector 3 for three fresh fuel enrichments including the 12 enriched poison Gd rods (1.68%, 0.80%, and 0.22% ^{235}U)

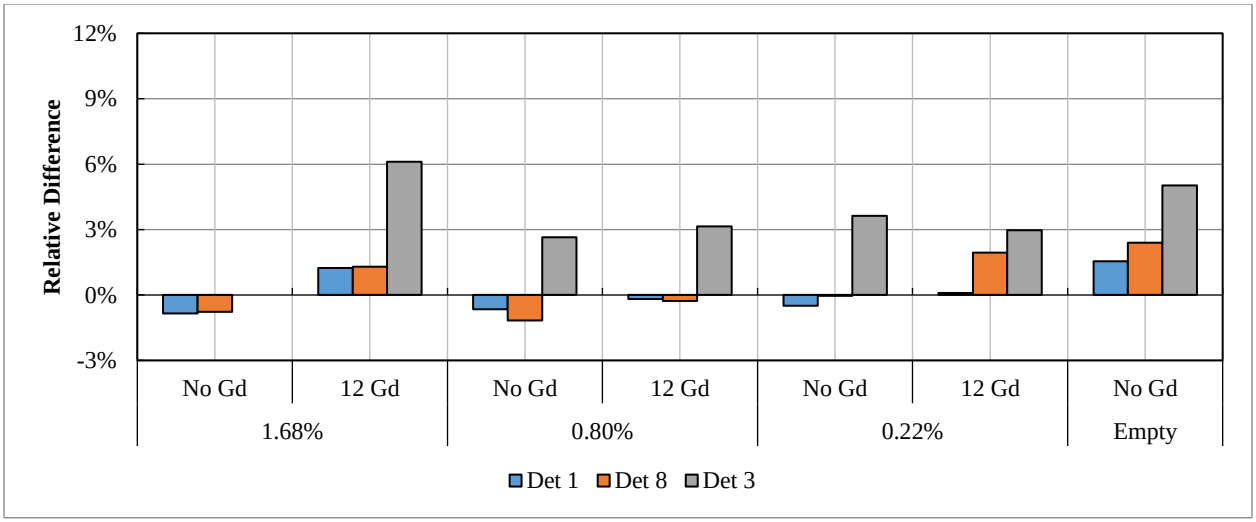

Figure 25 The relative differences between the experimental and simulated die-away times in the 70-100 μs time domain for detectors 1, 8, and 3 for several fresh fuel enrichments (with and without the Gd poison rods) were determined. There was no data available for Detector 3 for the 1.68% ^{235}U "No Gd" case.

Effect of Rod Substitution

A series of experiments was performed to determine the sensitivity of the system to the removal or replacement of LEU rods with DU rods. The simulated diversion scenarios consisted of removing 10 fresh LEU fuel rods (3.19% ^{235}U) and replacing them with 10 natural rods (0.72% ^{235}U), depleted rods (0.22% ^{235}U), or stainless steel (SS) rods. The positions of the fuel pin replacements were kept constant for each fuel assembly enrichment. The location of the fuel pin diversions were distributed throughout the assembly and are shown in blue in Figure 26**Error! Reference source not found.**. The DDA signal of the No Diversion case was compared to the 10 LEU pin diversion scenarios using NU, DU, and SS replacement pins. The dynamic evolutions of

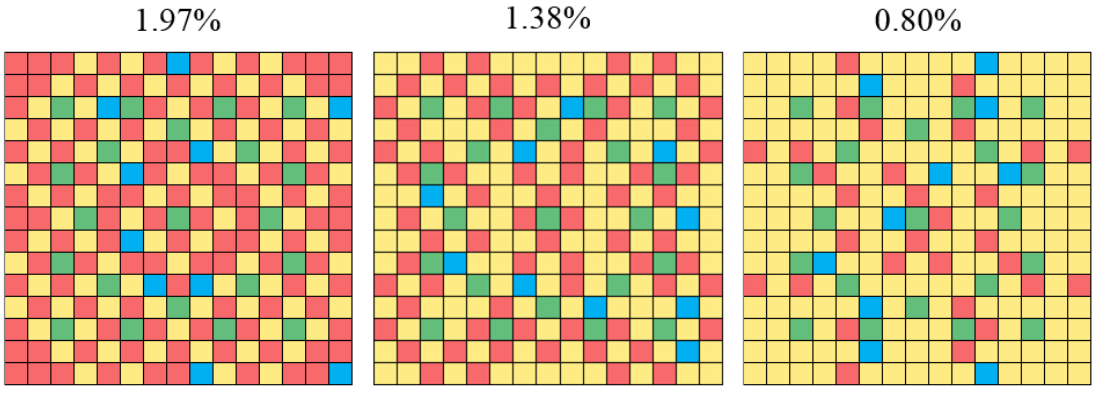

Figure 26 The schematics of the fresh fuel diversions, with red = LEU fuel rod, blue = Diversion position (natural, depleted, or stainless steel rod), yellow = DU, and green = Guide Tube. For the No Diversion scenario, blue = LEU.

the DDA signals for three different enrichments (1.97%, 1.38%, and 0.80% ^{235}U) were plotted for a Front (close to neutron generator) and Back (furthest from neutron generator) detector position

(Figure 27). Qualitatively, the three 10 pin replacement scenarios showed statistically significant differences compared to the No Diversion case. Removing small amounts of fissile material in increments (from NU to stainless steel) resulted in a decrease in the DDA signal and faster die away of the neutron population.

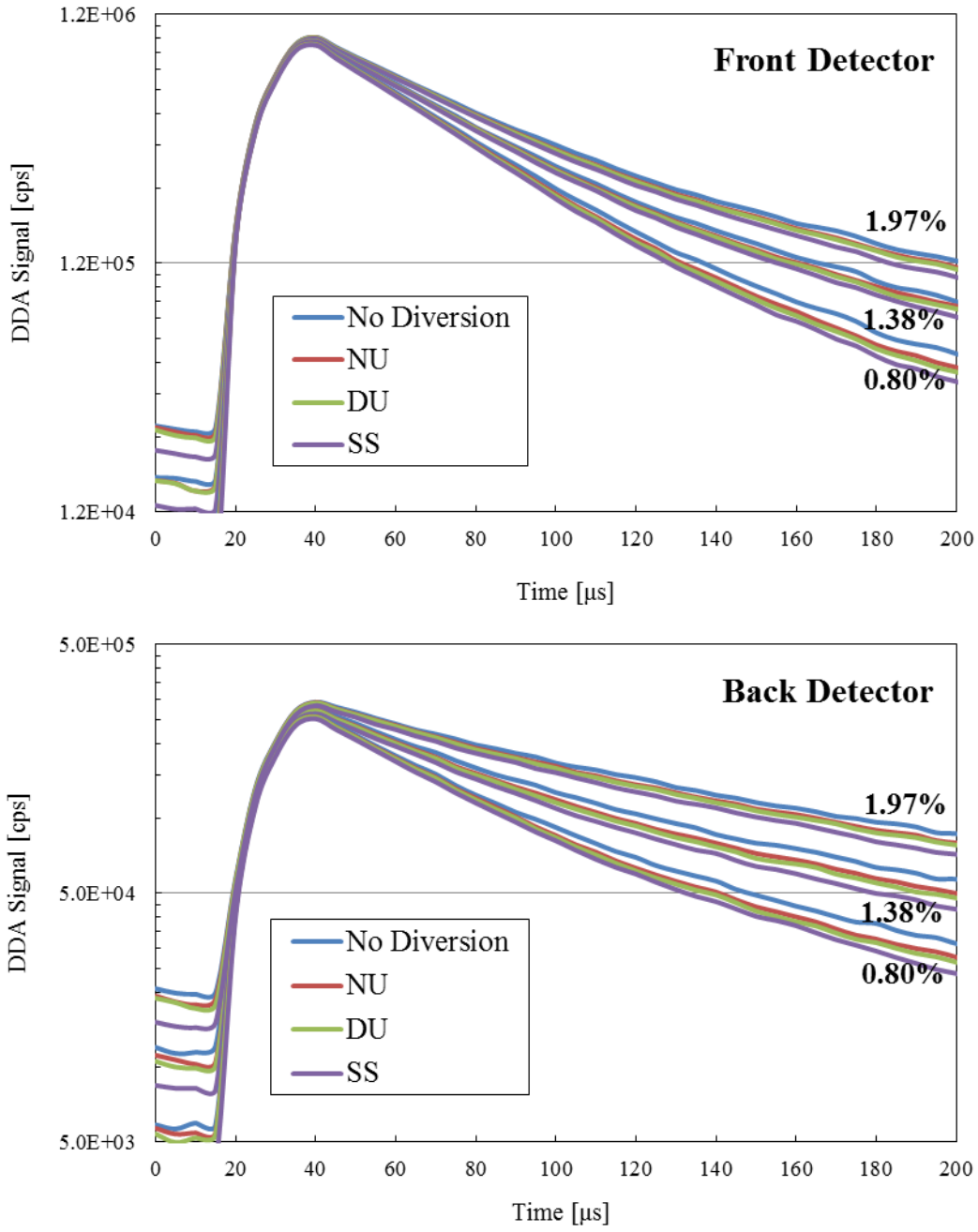

Figure 27 The dynamic evolution of the No Diversion (blue) DDA signal was observably affected by the three 10 pin replacement (NU, DU, and SS) scenarios for three different enrichments (1.97%, 1.38%, and 0.80% 235U) for detectors in the Front and Back (relative to the neutron generator).

For a quantitative comparison, the No Diversion DDA signals in the 70-100 μs time domain for Front and Back detectors were summed and compared to the summed DDA signals of the three

diversion scenarios (NU, DU, and SS rods). The relative differences between the No Diversion and diversion scenarios were determined for the three enrichments (Figure 28). The Back detectors (furthest from the neutron generator) showed a larger relative difference in the summed DDA signal than the Front detectors, with the differences ranging from 4-10% and 2-5%, respectively, for the NU, DU, and SS cases. The larger impact on the Back detectors is due to their increased sensitivity to the overall fuel assembly fissile content, while the Front detectors are more sensitive to local changes.

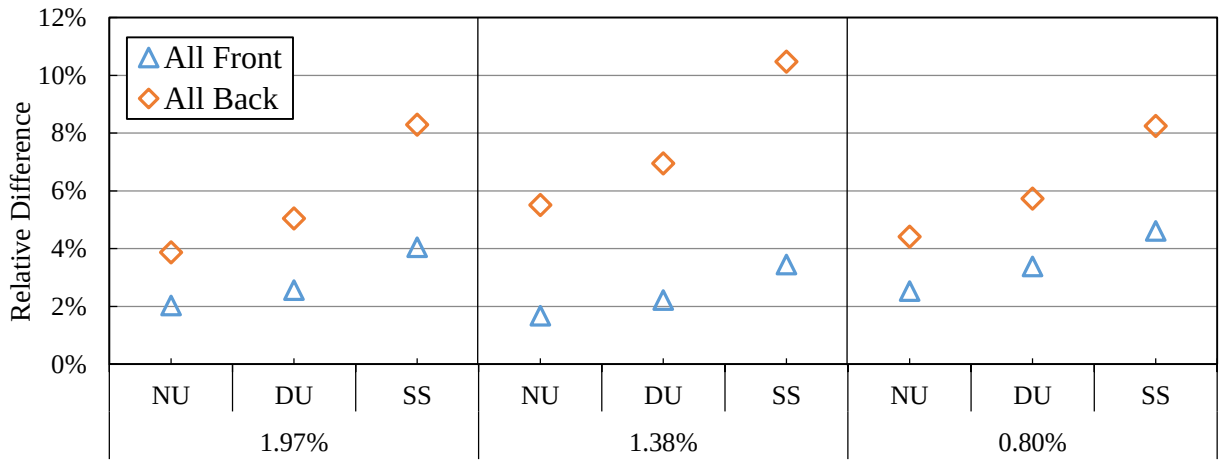

Figure 28 The relative difference of the integral of the DDA signal in the 70-100 μs time domain between the No Diversion case and the three 10 pin diversion cases (NU, DU, and SS rods) in the Front and Back detectors were determined. Overall, the back detectors were determined. Overall, the back detectors were more sensitive to changes in the fissile content of the assembly

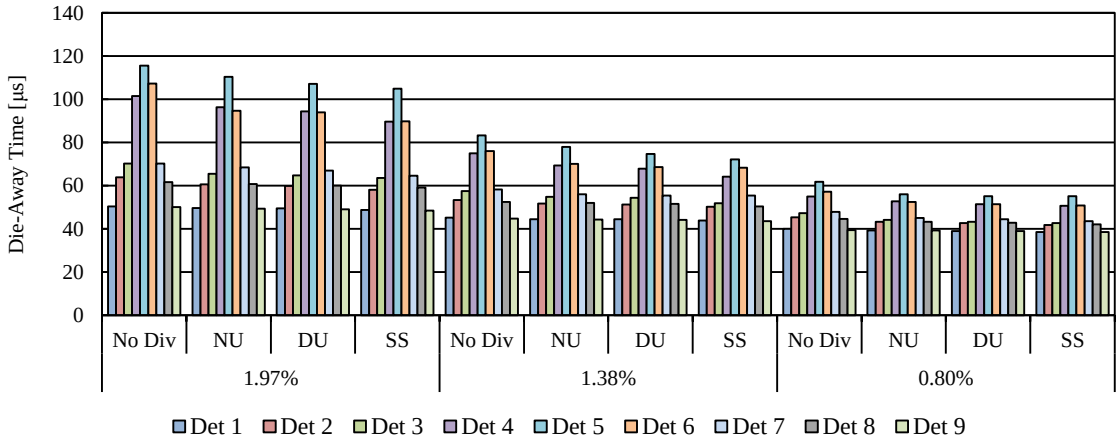

Figure 29 The DDA signal die-away times in the 70-100 μs time domain were determined for nine detectors, three enrichments, and four simulations (No Diversion, NU, DU, and SS)

The DDA signal die-away times in the 70-100 μs time domain were determined for all nine detectors for the three enrichments for the four simulations (No Diversion, NU, DU, and SS). The characteristic "Empire State" shape was observed, showing that the enrichment and detector position relative to the neutron generator impact the DDA signal die-away time (Figure 29). The relative differences between the No Diversion die-away time and the 10 pin replacement scenario die-away times were determined for the Front and Back detectors. The relative differences in die-away time ranged from approximately 2-9% for the

Front detectors and 4-16% for the Back detectors. Again, the back detectors were more sensitive to changes in the overall fissile content in the fuel assembly.

The results presented here suggest that sparse replacement of only 10 LEU fuel rods with a variety of materials containing less or no fissile material impacts the DDA instrument observables in a statistically significant manner. The amount of fissile material in the fuel assembly and the detector position clearly affect the recorded DDA signal and die-way time. There were significant changes to the DDA signal (4-10% on the Back detectors, 2-5% for the Front detectors relative to the No Diversion case) and die-away time (4-16% for the Back detectors, 2-9% for the Front detectors relative to the No Diversion case) due to the change in fissile content in the fuel assembly after replacing 10 LEU pins with 10 natural uranium, depleted uranium, or stainless steel fuel rods. In the case of the fresh fuel, the overall fissile content of the fuel is well known from the manufacturing process, allowing the detection of removed or replaced pins directly without the need for a reference measurement.

Source Tailoring

A simulation study was made of material that could be used to 'tailor' the neutron spectrum before it entered the fuel assembly. The purpose of this tailoring is to reduce the average energy of the interrogating neutron (intended to reduce fission in ^{238}U) and also to reduce the direct contribution of the neutron generator source neutrons in the detectors and so reduce background. Details of the study are given in reference A.14.

The results suggest that the presence of source neutron tailoring material does not substantially influence the DDA signal, as represented by the fission-to-burst and fission-to-source ratios evaluated for a wide range of commonly available materials (tungsten, lead, iron, water, and air) of different, yet practical, thicknesses (2-8 cm). Based on the calculation of the newly proposed figure of merit, we expect that the overall signal-to-background ratio can be improved by less than a factor of 2 when comparing the most (8 cm thick tungsten) and the least (air) effective tailoring material configurations.

But our results indicate that the choice of the tailoring material may significantly affect the fraction of fission chains that start with fission of ^{238}U which has previously been considered an undesired active background component distorting the measured DDA signal. We have therefore evaluated the performance of the DDA instrument in its ability to accurately reconstruct the effective fissile content of the SFA ($^{239}Pu_{eff}$) which is defined as the corresponding mass of ^{239}Pu that would give the same signal response as that obtained from all fissile isotopes (^{235}U, ^{239}Pu, and ^{241}Pu) in the fuel assembly. The effects of minimized and maximized ^{238}U first fission contribution were investigated in simulations by the presence or absence of source neutron tailoring material. The DDA instrument performance was simulated and compared for multiple NGSI-SF-created spent fuel libraries. Each spent fuel library represents a wide variety of fuel assemblies with different irradiation history, including varying IE, BU, and CT, position of the fuel in the nuclear reactor core, and density, temperature, and chemical composition of the moderator [11].

The results suggest that fission chains starting with fission on ^{238}U are a valid part of the DDA signal and do not negatively affect its quality; thus, fast fission on ^{238}U should no longer be considered an undesired part of the active background that needs to be minimized by the instrument design. In summary, the results of this study suggest that even though tailoring the energy of the source neutrons may help improve the overall performance of the DDA instrument, it should not be considered a critical design factor.

Generic DDA design

The NGSI spent fuel project is building a DDA instrument (including lessons learned from this project) as a dedicated, facility specific instrument for measurement in the temporary storage facility in Sweden. This current project included a study of potential conceptual designs that would allow the DDA technique were to be applied more generally in spent fuel ponds. The results are described in detail in reference A.6 and are summarized here.

Three preliminary Differential Die-Away (DDA) instrument designs are proposed for an underwater, non-destructive assay active neutron interrogation technique. Each design includes a justification and evaluation of the design parameters, including the pros and cons of each configuration.

One overarching design idea was to model the universal DDA instrument after another widely accepted safeguards instrument, the Fork Detector [7]. In pursuit of this goal, we adopted a design basis similar to the Fork Detector, except with the addition of the DT neutron generator in one of the arms positioned around the fuel assembly.

Design 1: 2-Sided with Vertical Neutron Generator

The initial idea of a general-use DDA instrument was to position the DT neutron generator vertically on one arm of the fork detector design with multiple neutron detectors placed inside of the other fork arm and back (Figure 30). The spent fuel assembly is surrounded by six neutron detectors, modeled as ^{3}He, which are shielded with several centimeters of Pb or W. The neutron generator, also shielded with Pb or W, stands vertically on a third side of the spent fuel assembly, such that the detectors are positioned at the "front" and "back" of the spent fuel assembly. The electronics for the detectors and control box for the neutron generator are also shielded behind the Pb or W frame.

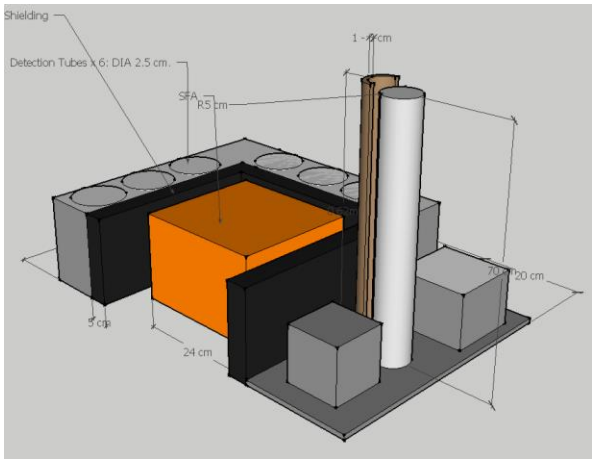

Figure 30 DDA Design 1 schematic with a vertically positioned DT neutron generator and two set of neutron detectors shielded by W or Pb in a fork-like detector design

Design 2: 2-Sided with Horizontal Neutron Generator

The Design 2 idea was conceived when attempting to reduce the amount of shielding required along the length of the DT neutron generator and maintain a fork-like detector design. In Design 2 the neutron generator is positioned horizontally relative to the spent fuel assembly with a cylindrical W or Pb shield surrounding the end of the generator close to the fuel assembly (Figure 31). The spent fuel assembly is surrounded by six neutron detectors, modeled as ^{3}He, which are shielded with blocks of Pb or W.

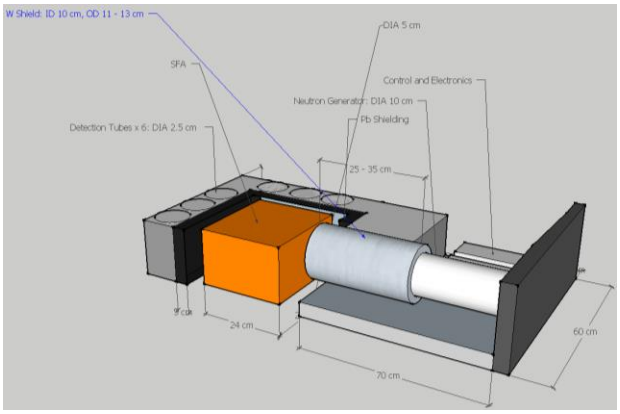

Figure 31 DDA Design 2 schematic with a horizontally positioned DT neutron generator and two set of neutron detectors shielded by W or Pb in a fork-like detector design

Design 3: 3-Sided with Mounted Neutron Generator

Design 3 was a significant change from our previous general-use DDA designs. Instead of incorporating the DT neutron generator into one of the fork detector arms, the neutron generator is mounted underwater to the side of the cooling pool wall. A spent fuel assembly would then be lifted by a crane into position in front of the neutron generator. A fork-like detector, including the ^{3}He or fission chambers, electronics, and gamma shielding material would be positioned around the fuel assembly in front of the neutron generator. To approach the neutron generator head on, the inspector would potentially need to stand on a bridge spanning the cooling pool. A design change would instead rotate the interrogation direction by 90°, thereby positioning the fuel assembly also adjacent to the cooling pool wall (Figure 32). This would allow the separate fork-like detector to approach the fuel assembly from the side and permit the inspector to stand on the side of the cooling pool wall thereby consolidating all of the underwater cables.In this configuration, the mass of the neutron generator, electronics, and majority of the Pb or W shielding material can be attached to the side of the pool wall and reduce the overall weight of the fork-like detector. Previously, our main issue was the heavy weight of the fork-like design as it was too massive for a 2 person team to maneuver. With the separated design, the majority of the weight on the hand-maneuvered fork-like detector is reduced, therefore allowing for easier handling of the instrument.

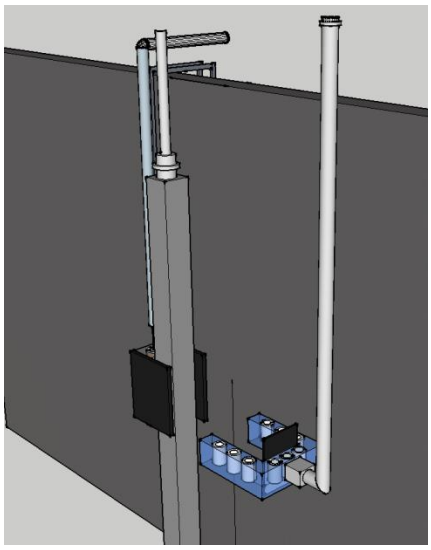

Figure 32 DDA Design 3 with the direction of interrogation rotated 90° to allow the inspectors to stand by the side of the cooling pool wall.

The active, non-destructive assay DDA instrument for spent nuclear fuel characterization has the potential to be a robust nuclear safeguards technique. These preliminary general-use DDA instrument designs represent a variety of design evolutions being considered at Los Alamos National Laboratory. We plan to continue to refine our general-use DDA designs.

Overall, the main design hurdles were keeping the mass of the instrument low such that it could be reasonably handled by a team of 1-2 inspectors. This led to the most promising Design 3 configuration, with the wall-mounted DT neutron generator and a separate fork-like detector.

Although the detection head considered here is very similar to the current fork detector, an additional design idea being considered is to potentially test the Design 3 general-use DDA instrument using an actual, off-the-shelf Fork Detector, consisting of four fission chambers. Using an off-the-shelf instrument as the detector component would give less spatial information about the fuel assembly by would be a less expensive way to test the potential capabilities of the general-use DDA instrument. Of course a separate waterproof, shielded, wall-mounted DT neutron generator container would need to be constructed and installed using a crane at the test facility.

Conclusions

The objective of this work was to move the DDA technique for spent fuel from Monte Carlo simulations to a practical instrument. The work is composed of two parts: i) demonstrating a practical DDA measurement system and ii) confirming that simulations closely represented reality.

Successful demonstration of the technique

We have demonstrated a complete system of neutron interrogation, detection and data acquisition with a neutron generator of the appropriate strength for spent fuel applications.

- Thermo-Fisher neutron generator minimum pulse width 5% duty cycle – not like older generation running with 10μs wide pulses at 100Hz
- Tested the performance of faster post-burst recovery electronics and different detector types
- Measured 14 MeV neutron generator strength with Nb foil activation
- ^{238}U fast flux monitor tested

The lessons we have learned from this project have been incorporated in the design of the NA24 DDA instrument to be used in CLAB in Sweden.

One caveat is that these tests were carried out under very low gamma dose rates. This is unlike the spent fuel application. For the NA24 DDA design a conservative approach of using lead shielding will be used to reduce the gamma dose rates at the detector location to low levels (~20R/hr).

Confirmation of Simulations

We have performed Monte Carlo simulations of our experimental setup, which includes all of the features that are important to neutron transport behavior. We also included sensitivity studies of the DDA response to key model parameters in order to obtain a realistic total uncertainty estimate. Overall, we found good agreement between the experiment and simulation, with the relative difference (~3%) between the die-away time results within uncertainty (~5%). The uncertainty on the die-away time is dependent on statistical variation in the exponential fit (<1%) and small discrepancies between the experimental setup and simulation geometry (up to 5%). Other uncertainties affecting the DDA signal magnitude include the DT neutron generator yield and the absence of delayed neutrons in the simulations. The die-away time comparison has less uncertainty than the absolute signal strength because it is independent of the absolute neutron generator strength but is still affected by the uncertainty in the deadtime correction coefficient, particularly for the front detectors in the early time period.

This agreement gives confidence in the Monte Carlo predicted performance of the real instrument. Although using the less complex fresh fuel (but supplemented by thermal neutron absorbers), this study confirms general trends reflecting the overall physics of the DDA instrument as previously identified through spent fuel simulation, which assumes that the dynamic evolution of the DDA signal reflects the effective fissile and neutron absorber content, not a particular isotopic composition. These results therefore support conclusions derived from simulations of spent fuel assay which predict the capabilities of the DDA instrument to characterize spent fuel for nuclear safeguards applications.

Acknowledgement

This work was funded by the Defense Nuclear Nonproliferation Office of Nonproliferation and Verification Research and Development.

References

1. S.J. Tobin et al. “Technical Cross-Cutting Issues for the Next Generation Safeguards Initiative’s Spent Fuel Nondestructive Assay Project” JNMM special edition April 2012
2. S.J. Tobin et al. “Quantifying the Plutonium Mass in Spent Fuel Assemblies with Nondestructive Assay – An update on the NGSI Research Effort” Proc. INMM annual meeting Palm Desert 2011.
3. S. J. Tobin, H. O. Menlove, M. T. Swinhoe and M. A. Schear “Next Generation Safeguards Initiative research to determine the Pu mass in spent fuel assemblies: Purpose, approach, constraints, implementation and calibration” Nucl. Instr. Methods A652 (2011) 73-75
4. Vladimir Henzl, Martyn T. Swinhoe, Stephen J. Tobin, and Howard O. Menlove “Determination of Pu content in a Spent Fuel Assembly by Measuring 244Cm content and Multiplication with the Differential Die-Away Instrument.” INMM conference 2012 Orlando.
5. Vladimir Henzl, Martyn T. Swinhoe, Stephen J. Tobin, Howard O. Menlove, Jack Galloway and Dong Won Lee “*Direct Measurement of Initial Enrichment, Burn-up and Cooling Time of Spent Fuel Assembly with a Differential Die-Away Technique Based Instrument.*” INMM conference 2012 Orlando.
6. J.D. Chen, A.F. Gerwing, R. Keeffe, M. Larsson, K. Jansson, L. Hildingsson, B. Lindberg, E. Sundkvist, U. Meijer, M. Thorsell, and M. Ohlsson, “*Long-Cooled Spent Fuel Verification Using a Digital Cerenkov Viewing Device*,” International Atomic Energy Agency report IAEA-SM-367/14/07 (2007).
7. P.M. Rinard and G.E. Bosler, “Safeguarding LWR Spent Fuel with the Fork Detector,” Los Alamos National Laboratory report LA-11096-MS (1988).
8. A. Lebrun, M. Merelli, J-L. Szabo, M. Huver, R. Arlt, and J. Arenas-Carrasco, “*SMOPY a New NDA Tool for Safeguards of LEU and MOX Spent Fuel*,” International Atomic Energy Agency report IAEA-SM-367/14/03 47 (2003).
9. Robert C. Runkle, David L. Chichester, Scott J. Thompson. *“Rattling nucleons: New developments in active interrogation of special nuclear material”* Nuclear Instruments and Methods in Physics Research A 663 (2012) 75–95
10. D. Pelowitz and et al, "MCNPX User's Manual, Version 2.7.0," Los Alamos National Laboratory, LA-UR-11-00438, 2011.
11. H. Trellue, J. Galloway, N. Fischer and S. Tobin, "Advances in Spent Fuel Libraries," in *Proceedings of Institute of Nuclear Materials Management conference*, Palm Desert, CA, 2013.

APPENDIX I Publications, Report and Presentations funded, or partially funded, by this project

A.1 Martinik, Tomas ; Henzl, Vladimir ; Grape, Sophie ; Jansson, Peter ; Swinhoe, Martyn Thomas; Goodsell, Alison Victoria ; Tobin, Stephen Joseph "D*evelopment of a Differential Die-Away Instrument for Characterization of Swedish Spent Nuclear Fuel"* ESARDA Symposium - 37th Annual Meeting ; 2015-05-19 - 2015-05-21 ; Manchester, United Kingdom LA-UR-15-23345 2015-06-22

A.2 Goodsell, Alison Victoria; Henzl, Vladimir; Swinhoe, Martyn Thomas; Charlton, William Smith *"Simulation Study for Detection of Pin Diversion with the Differential Die-Away Instrument Using Fresh Fuel"* Institute of Nuclear Materials Management 56th Annual Meeting ; 2015-07-12 - 2015-07-16; Indian Wells, California, United States LA-UR-15-24112 2015-12-15

A.3 Swinhoe, Martyn Thomas; Goodsell, Alison Victoria; Henzl, Vladimir; Desimone, David J. ; Rael, Carlos D.; Ianakiev, Kiril Dimitrov; Iliev, Metodi, **"***Development of Techniques for Spent Fuel Assay"* Nuclear Weapons and Materials Security Portfolio Review; 2015-03-17 - 2015-03-17 ; Livermore, California, United States LA-UR-15-21448 2015-03-18

A.4 Goodsell, Alison Victoria; Swinhoe, Martyn Thomas; Henzl, Vladimir, Rael, Carlos D.; Desimone, David J. ***"****Differential Die-Away Instrument: Report on Benchmark Measurements and Comparison with Simulation for the Effects of Neutron Poisons"* LA-UR-15-22259 2015-03-30

A.5 Tobin, Stephen Joseph; Lundkvist, Niklas; Goodsell, Alison Victoria; Grape, Sophie; Hendricks, John S.; Henzl, Vladimir; Swinhoe, Martyn Thomas **"***A Qualitative Analysis of the Neutron Population in Fresh and Spent Fuel Assemblies during Simulated Interrogation using the Differential Die-Away Technique"* LA-UR-15-23441 2015-05-06

A.6 Goodsell, Alison Victoria; Trujillo, Estevan Rey; Henzl, Vladimir; Swinhoe, Martyn Thomas ***"****Report on Conceptual Study of In-field Differential Die-Away Instrument"* LA-UR-15-25942 2015-07-29

A.7 Martinik, Tomas; Henzl, Vladimir; Swinhoe, Martyn Thomas; Grape, Sophie; Jansson, Peter; Goodsell, Alison Victoria; Tobin, Stephen Joseph ***"****Design of a Prototype Differential Die-Away Instrument proposed for Swedish Spent Nuclear Fuel Characterization"* LA-UR-15-28331 2015-10-26

A.8 Goodsell, Alison Victoria; Ianakiev, Kiril Dimitrov; Iliev, Metodi; Swinhoe, Martyn Thomas; Henzl, Vladimir; Desimone, David J. ***"*** *Report on Optimized Neutron Detector Performance"* LA-UR-15-29538 2015-12-15

A.9 Goodsell, Alison Victoria; Swinhoe, Martyn Thomas; Henzl, Vladimir; Ianakiev, Kiril Dimitrov; Iliev, Metodi; Rael, Carlos D. ; Desimone, David J. ***"****Differential Die-Away Instrument: Comparison of MCNPX Simulations to Benchmark Experiment"* IEEE NUCLEAR SCIENCE SYMPOSIUM & MEDICAL IMAGING CONFERENCE 21ST SYMPOSIUM ON ROOM-TEMPERATURE SEMICONDUCTOR X-RAY AND GAMMA-RAY DETECTORS; 2014-11-08 - 2014-11-15; Seattle, Washington, United States LA-UR-14-28387 2014-10-28

A.10 Goodsell, Alison V., Swinhoe, Martyn T.; Henzl, Vladimir; Rael, Carlos D.; Desimone, David J., **"***Development of Techniques for Spent Fuel Assay"* Office of Defense Nuclear Nonproliferation Research & Development Detection, Emergency Response, Safeguards, Radiological Source Replacement, Arms Control and Enabling Capabilities Program Review WMS 2014 ; 2014-05-20 - 2014-05-20 ; Lemont, Illinois, United States LA-UR-14-23035 2014-04-30

A.11 Goodsell, Alison V.; Swinhoe, Martyn T.; Henzl, Vladimir; Ianakiev, Kiril D.; Iliev, Metodi; Rael, Carlos D.; Desimone, David J. ***"****Differential Die-Away Instrument: Benchmarking of Monte Carlo to Experiment"* IEEE Nuclear Science Symposium & Medical Imaging Conference ; 2014-11-08 - 2014-11-08 ; Seattle, Washington, United States LA-UR-14-23172 2014-05-05

A.12 Goodsell, Alison Victoria; Swinhoe, Martyn Thomas ; Henzl, Vladimir ; Charlton, William Smith, ***"****An Overview of the Differential Die-Away Instrument Fresh PWR Fuel Experiments and Comparison to MCNPX Simulations for Nuclear Safeguards Applications"* American Nuclear Society Student Conference ; 2015-04-09 - 2015-04-11 ; College Station, Texas, United States LA-UR-15-21691 2015-03-09

A.13 Goodsell, Alison Victoria; Henzl, Vladimir; Swinhoe, Martyn Thomas; Rael, Carlos D.; Desimone, David J.; Charlton, William Smith **"***Comparison of fresh fuel experimental measurements to MCNPX results using the differential die-away instrument for nuclear safeguards applications"* ESARDA Symposium 2015 37th Annual Meeting ; 2015-05-18 - 2015-05-18 ; Manchester, United Kingdom LA-UR-15-23252 2015-04-30

A.14 Goodsell, Alison Victoria; Henzl, Vladimir; Swinhoe, Martyn Thomas ***"****The Impact of Tailoring the Interrogating Neutron Energy Spectrum on the Performance of the Differential Die-Away Instrument during Spent Fuel Assay"* LA-UR-15-28345 2015-10-26

A.15 Goodsell, Alison Victoria; Swinhoe, Martyn Thomas; Henzl, Vladimir; Rael, Carlos D.; Desimone, David J. **"***Differential Die-Away Instrument: Report on Fuel Assembly Mock-up Measurements with Neutron Generator"* LA-UR-14-27305 2014-09-18

A.16 Goodsell, Alison Victoria; Swinhoe, Martyn Thomas; Henzl, Vladimir; Ianakiev, Kiril Dimitrov ; Iliev, Metodi; Rael, Carlos D.; Desimone, David J. **"***Differential Die-Away Instrument: Report on Neutron Detector Recovery Performance and Proposed Improvements"*
LA-UR-14-27369 2014-09-22

A.17 Goodsell, Alison Victoria "*NA-22 DDA Instrument NGSI-SF Project Annual Meeting"* NGSI-SF Project Annual Meeting; 2014-11-18 - 2014-11-18; Los Alamos, New Mexico, United States LA-UR-14-28967 2014-11-19

A.18 Goodsell, Alison Victoria; Henzl, Vladimir; Swinhoe, Martyn Thomas; Rael, Carlos D.; Desimone, David J. **"***Differential Die-Away Instrument: Report on Comparison of Fuel Assembly Experiments and Simulations"* LA-UR-15-20242 2015-01-14

A.19 Ianakiev, Kiril D.; Swinhoe, Martyn T.; Iliev, Metodi; Goodsell, Alison V. **"***New-Generation Thermal Neutron Detectors and Electronics for High-Count-Rate Applications"* LA-UR-14-23377 2014-05-13

A.20 Goodsell, Alison V.; Henzl, Vladimir; Swinhoe, Martyn T. ***"****Differential Die-Away Instrument: Report on Initial Simulations of Spent Fuel Experiment"*LA-UR-14-22162 2014-04-01

A.21 Swinhoe, Martyn Thomas; Goodsell, Alison Victoria; Desimone, David J.; Henzl, Vladimir; Rael, Carlos D. "*FY14 Annual Report DEVELOPMENT OF TECHNIQUES FOR SPENT FUEL ASSAY"* LA-UR-14-27828 2014-10-07